Comparison of MISR and Meteosat-9 cloud-motion vectors

Katrin Lonitz[1,2] and Ákos Horváth[3,4]

Received 31 March 2011; revised 27 October 2011; accepted 27 October 2011; published 24 December 2011.

[1] Stereo motion vectors (SMVs) from the Multiangle Imaging SpectroRadiometer (MISR) were evaluated against Meteosat-9 cloud-motion vectors (CMVs) over a one-year period. In general, SMVs had weaker westerlies and southerlies than CMVs at all latitudes and levels. The E-W wind comparison showed small vertical variations with a mean difference of -0.4 m s^{-1}, -1 m s^{-1}, -0.7 m s^{-1} and corresponding rmsd of 2.4 m s^{-1}, 3.8 m s^{-1}, 3.5 m s^{-1} for low-, mid-, and high-level clouds, respectively. The N-S wind discrepancies were larger and steadily increased with altitude, having a mean difference of -0.8 m s^{-1}, -2.9 m s^{-1}, -4.4 m s^{-1} and rmsd of 3.5 m s^{-1}, 6.9 m s^{-1}, 9.5 m s^{-1} at low, mid, and high levels. The best overall agreement was found in marine stratocumulus off Namibia, while differences were larger in the Tropics and convective clouds. The SMVs were typically assigned to higher altitudes than CMVs. Attributing each observed height difference to MISR and/or Meteosat-9 retrieval biases will require further research; nevertheless, we already identified a few regions and cloud types where CMV height assignment seemed to be the one in error. In thin mid- and high-level clouds over Africa and Arabia as well as in broken marine boundary layer clouds the 10.8-μm brightness temperature-based heights were often biased low due to radiance contributions from the warm surface. Contrarily, low-level CMVs in the South Atlantic were frequently assigned to mid levels by the CO_2-slicing method in multilayer situations. We also noticed an apparent cross-swath dependence in SMVs, whereby retrievals were less accurate on the eastern side of the MISR swath than on the western side. This artifact was traced back to sub-pixel MISR co-registration errors, which introduced cross-swath biases in E-W wind, N-S wind, and height of 0.6 m s^{-1}, 2.6 m s^{-1}, and 210 m.

Citation: Lonitz, K., and Á. Horváth (2011), Comparison of MISR and Meteosat-9 cloud-motion vectors, *J. Geophys. Res.*, *116*, D24202, doi:10.1029/2011JD016047.

1. Introduction

[2] Horizontal motion vectors, or 'winds', are routinely derived by tracking cloud patterns in geostationary imagery or overlapping swaths of polar radiometers [*Schmetz et al.*, 1993; *Turner and Warren*, 1989; *Key et al.*, 2003]. These cloud-motion vectors (CMVs) have reached the maturity to positively impact global forecasts when assimilated into numerical weather prediction (NWP) systems [*Rohn et al.*, 2001; *Bormann and Thépaut*, 2004]. Nonetheless, there is room for CMV improvements both in terms of accuracy and spatial coverage. The largest source of uncertainty restricting the use of traditional CMVs is height assignment, which relies on interpreting the cloud radiometric signature in the infrared window, CO_2, or water vapor channels with the help of radiative transfer calculations and forecast temperature profiles. Operational algorithms can have prohibitively large height errors up to 3 km. An additional limitation is the scarcity of CMVs in the 55°-65° latitude band, poleward of geostationary and equatorward of polar orbiter coverage.

[3] A complementary data set of stereo motion vectors (SMVs) from MISR (Multiangle Imaging SpectroRadiometer) might mitigate these shortcomings. The novel MISR stereo algorithm simultaneously derives mesoscale winds and heights by matching cloud reflectivity patterns from three different view angles [*Horváth and Davies*, 2001a]. Because the technique is purely geometric and self-contained with no need for ancillary data, SMV heights are potentially more accurate than traditional CMV heights. Due to its sun-synchronous polar orbit, MISR also allows the global sampling of winds including the data-sparse area at high latitudes, albeit with poor temporal resolution.

[4] However, before SMVs could be used to address the shortcomings of traditional winds, SMV errors must be fully characterized. Such an evaluation is needed regardless of possible NWP applications, because accurate mesoscale SMVs are integral to the derivation of the flagship MISR product of high-resolution cloud top heights (CTHs). SMV

[1]Department of Physics and Geoscience, University of Leipzig, Leipzig, Germany.
[2]Now at Atmosphere in the Earth System, Max Planck Institute for Meteorology, Hamburg, Germany.
[3]Atmosphere in the Earth System, Max Planck Institute for Meteorology, Hamburg, Germany.
[4]Now at Satellite Remote Sensing Group, Physics Department, Leibniz Institute for Tropospheric Research, Leipzig, Germany.

0148-0227/11/2011JD016047

biases are in fact the dominant error source of CTHs as shown by *Marchand et al.* [2007] and *Ludewig* [2010].

[5] Unfortunately, quantitative assessments of MISR SMVs are few. Prelaunch estimates from simulated data indicated an RMS uncertainty of ~4 m s^{-1} for wind and ~400 m for height [*Horváth and Davies*, 2001a]. Soon after launch, *Horváth and Davies* [2001b] reported a qualitative comparison to GOES-10 (Geostationary Operational Environmental Satellite) CMVs in a case study of one extratropical cyclone. MISR wind and height retrievals were consistent with the synoptic situation and visually agreed well with geostationary CMVs; however, no quantitative assessment was offered.

[6] *Marchand et al.* [2007] conducted a limited comparison to radar wind profiler data at the ARM SGP (Atmospheric Radiation Measurement Program Southern Great Plains) site, including ~100 matched wind pairs. As predicted during the design of the retrieval algorithm [*Horváth and Davies*, 2001a], the MISR north-south (N-S) wind component was found significantly more uncertain than the east-west (E-W) wind component with a standard deviation of 13 m s^{-1} versus 5.5 m s^{-1}. However, both components showed small biases of 1–2 m s^{-1}.

[7] Subsequent upgrades to the MISR wind retrieval algorithm, such as more accurate camera-to-camera co-registration and parallax assessment, as well as stricter quality control were implemented by *Davies et al.* [2007], who also compared the improved SMVs against 6-h model forecast winds from the GMAO (Global Modeling and Assimilation Office) data assimilation system, utilizing ~85,000 observations. The MISR speed bias was negligible for low-level and mid-level clouds, and was only 1 m s^{-1} for high-level clouds, but the corresponding RMS vector difference increased with altitude from 5 m s^{-1} to 7.4 m s^{-1} to 10.5 m s^{-1}. However, because the mean wind speed also increased with height, relative differences were actually smaller at upper levels.

[8] The latest assessment by *Hinkelman et al.* [2009] expanded the *Marchand et al.* [2007] study to 23 radar wind profiler sites located across the central United States, increasing the number of matched SMV – radar wind pairs to ~1,200. Similar to earlier results, they found poorer agreement for the north-south than the east-west wind component; however, the general comparison improved substantially since *Marchand et al.* [2007] with typical biases of ~1.3 m s^{-1} and standard deviations of 4–6 m s^{-1}. Standard deviations also increased with height but relative to mean wind speeds they were smaller at higher altitudes, as in the findings of *Davies et al.* [2007]. Overall, *Hinkelman et al.* [2009] confirmed that tightening MISR quality control significantly improved SMVs, although at the expense of greatly reduced coverage.

[9] The purpose of our paper is to advance the error characterization of MISR SMVs via comparison to state-of-the-art Meteosat-9 geostationary CMVs. Geostationary winds are a more mature product with better-characterized errors than MISR winds. The operational CMVs are also successfully assimilated in NWP; therefore, they do set the stage for the evaluation of the still experimental SMVs. Nevertheless, we present our comparison results as *differences* and only refer to *biases* when the source of the observed disagreements is attributable with some confidence to one or the other of the data sets. The analysis uses one year of data and comprises ~225,000 wind pairs, far exceeding earlier studies. This large sample number allows us to obtain statistically significant results on unexplored aspects of MISR winds, such as their spatial error distribution. Another goal is to identify geographic regions where SMV heights can provide corrections to CMV heights and, thus, might have a positive forecast impact.

[10] The paper is organized as follows. Section 2 describes the two wind algorithms, the accuracy and NWP usage of CMVs, and the comparison method. Section 3 contains an analysis of MISR cloud-free ground retrievals. Section 4 offers a detailed account of SMV-CMV differences, including a case study in marine boundary layer clouds. Finally, section 5 summarizes our results and outlines future efforts to produce SMVs suitable for NWP purposes.

2. Data and Comparison Method

2.1. MISR SMV Retrieval Algorithm

[11] Full details of the stereo algorithm are provided by *Diner et al.* [1999], *Horváth and Davies* [2001a], and *Davies et al.* [2007]; here, only a summary is given. The MISR instrument on the Terra satellite measures the reflected solar radiation of a given scene at nine different angles within a 7-min interval. Complementing the nadir (An) camera, four cameras point forward (f) (Df, Cf, Bf, Af) and four cameras aft (a) (Da, Ca, Ba, Aa) relative to the flight direction. The view angles of the oblique D, C, B, and A cameras are 70°, 60°, 46°, and 26°, respectively. MISR's blue, green, red, and near-infrared channels only allow daytime imaging with an equator crossing of 10:30 A.M. local solar time. Cloud retrievals use red band (672 nm) data available at ~275 m sampling.

[12] The flagship MISR cloud product is high-resolution (1.1 km) geometric cloud top heights (CTHs) derived from cloud displacement (parallax) between the nadir and Af or Aa cameras. Mesoscale (70.4 km) cloud motion was originally used only to remove the advection bias in these CTHs (a 1 m s^{-1} along-track wind results in an 80–90 m height error); however, it was later introduced as a separate product on its own merit. The unique feature of MISR is its ability to *simultaneously* determine the mesoscale horizontal wind and associated height. Note, vertical cloud motion is neglected, which can introduce significant errors in vigorous convective systems. The negative impact of this simplification, however, is limited because the area covered by active convective plumes is relatively small. Also note that the height produced by the wind retrieval is representative only at the 70.4-km scale and is not to be confused with the high-resolution CTHs. The algorithm is purely geometric and requires only two parallax measurements from three angles. Because of view geometry, the cross-track (east-west) parallax is mostly due to cloud motion, while the along-track (north-south) parallax is a combination of cloud motion and height. Consequently, wind is retrieved with higher accuracy in the cross-track direction than in the along-track direction, where cloud motion and height are strongly coupled. For each mesoscale domain, two stereo motion vectors are obtained by tracking cloud patterns separately in the forward Df/Bf/An and aft Da/Ba/An camera triplets. The reported SMV is the average of the forward and aft vectors.

[13] A key component of SMV retrieval is stereo matching, that is, identification of a given cloud pattern in multi-angle images [*Muller et al.*, 2002]. For wind retrieval, MISR currently uses the Nested Maxima feature matcher, which tracks local reflectance maxima. This matcher is fast but relatively noisy, thus, O(100) samples are required to accurately map the parallax field. In section 4.2, we will also test the more accurate M2/M3 area-based matcher, which is used operationally only in the high-resolution CTH retrievals due to its high computational cost. Neither of these matchers has true sub-pixel accuracy; however, a sub-pixel (floating point) parallax is estimated as the weighted average of the most populated bins in the integer parallax histogram [*Davies et al.*, 2007].

[14] Quality control assesses orbit navigation, parallax signal strength, and fwd-aft retrieval consistency, providing flags for entire orbits as well as for individual SMVs. Because the stereo technique is very sensitive to image co-registration errors, poorly registered orbits were excluded from our analysis (Orbit_QA or Orbit_qa_winds flag of −1). The quality of an individual SMV is characterized by the WindQuality (WQ) flag, which varies from 0 to 4 representing ever more stringent requirements on the fwd-aft differences in wind speed, height, and direction. Additional information about the quality of image co-registration and the failure or success of stereo matching is reported in the CloudMotionSource flag. Our final analysis was restricted to SMVs with a WindQuality of 3 ('good') or 4 ('very good') and CloudMotionSource ≥ 3, as per MISR product guidelines [http://eosweb.larc.nasa.gov/PRODOCS/misr/Quality_Summaries/L2_Cloud_Products.html].

[15] Last, a caveat is worth noting here. The MISR algorithm does not employ a priori target selection; therefore, retrieval is attempted for every 70.4×70.4 km^2 domain irrespective of the presence, or lack thereof, of clouds. In featureless clear-sky ocean scenes wind retrieval fails, however, in clear-sky land scenes the stereo matcher is able to track surface patterns, returning near-zero "wind" speed and the height of topography. Such ground retrievals are useful for putting minimum error bars on cloudy SMVs; however, they should not be included either in our comparison or in NWP applications. In section 3, we will give a detailed analysis of ground retrievals and develop a methodology to flag them in the MISR product.

2.2. Meteosat-9 CMV Retrieval Algorithm

[16] The theoretical basis and current operational status of the algorithm are provided by *EUMETSAT* [2011] and *Holmlund et al.* [2010]. This section offers a brief summary only. The Meteosat-9 CMVs used in the present study were derived from daytime visible and infrared imagery of the SEVIRI (Spinning Enhanced Visible and Infrared Imager) instrument. In each synoptic hour, SEVIRI acquires four images at 15-min intervals, from which three intermediate CMVs are computed. For NWP purposes the weighted averages of intermediate vectors are also reported, but these were not considered in our analysis.

[17] Unlike MISR, Meteosat-9 employs a priori target selection based on the cloud mask and contrast of 3×3-pixel regions. Selected cloud targets are then tracked in the 3-km nominal resolution imagery using an area-based cross correlation (or squared Euclidean distance) matcher. Sub-pixel matching is emulated similar to MISR, but here with a local polynomial fit to the pixel-resolution correlation (or Euclidean distance) surface. Meteosat-9 winds are representative of an area comparable to the MISR domain size: 72×72 km^2 at the sub-satellite point, which increases with view zenith angle and doubles at the limb.

[18] The most error prone step in CMV derivation is height assignment. (Note that height is only reported for final (hourly) CMVs and not for intermediate CMVs.) The default method matches the coldest measured infrared (10.8 μm) equivalent blackbody brightness temperature (EBBT) to an ECMWF (European Centre for Medium-Range Weather Forecasts) temperature profile. The EBBT approach works well for opaque clouds, however, for semitransparent or sub-pixel clouds two alternative techniques are employed. The CO_2-slicing method, usually applied above 650 hPa, equates measured and calculated ratios of infrared (10.8 and 12 μm) and CO_2 (13.4 μm) channel radiance differences [*Nieman et al.*, 1993]. The water vapor intercept method, usually applied above 400 hPa, is a conceptually similar technique but uses water vapor (6.2 and 7.3 μm) and infrared (10.8 μm) measurements in both clear sky and cloudy sky [*Schmetz et al.*, 1993]. Finally, for stratocumulus clouds one of two possible downward corrections is applied to the EBBT height. If the forecast profile indicates low-level temperature inversion, CMVs are assigned to the inversion height. In areas without temperature inversion, on the other hand, CMVs are assigned to an estimated cloud base height following the conceptual idea of *Le Marshall et al.* [1993]. This latter adjustment first separates the smoothed EBBT histogram into cloud and surface clusters. Cloud base EBBT is then determined as the cloud-cluster-mean EBBT plus the standard deviation of cloud cluster EBBTs multiplied by an amplitude factor.

[19] In general, all of the above height assignment methods are applied to each CMV. A single final height is then derived from the successfully executed methods by one of two ways. The nominal sequential technique uses a deterministic approach and selects the final height from a priority list of height assignment methods. Alternatively, the final height can be computed as the weighted mean of all valid height retrievals. Operational practice prefers the sequential method.

[20] The quality control scheme [*Holmlund*, 1998; *Holmlund et al.*, 2001] applies the following tests to both intermediate and final CMVs: (i) consistency with forecast winds, (ii) spatial vector and height consistency of neighboring CMVs, (iii) temporal vector, speed, direction, and height consistency of consecutive intermediate CMVs, and (iv) image correlation between the 10.8 μm and 6.2 μm channels. A final normalized quality indicator (QI) ranging 0–1 is then derived as the weighted mean of the consistency tests multiplied by the image correlation test. Following geostationary wind monitoring guidelines, we only used CMVs with a model-independent QI ≥ 0.8, which excluded the forecast consistency check [*Forsythe and Saunders*, 2008].

2.3. Meteosat-9 CMV Accuracy and Use in Numerical Weather Prediction

[21] Geostationary cloud motion winds are considerably more mature and have better error characterization than MISR SMVs. Therefore; it is useful to summarize typical

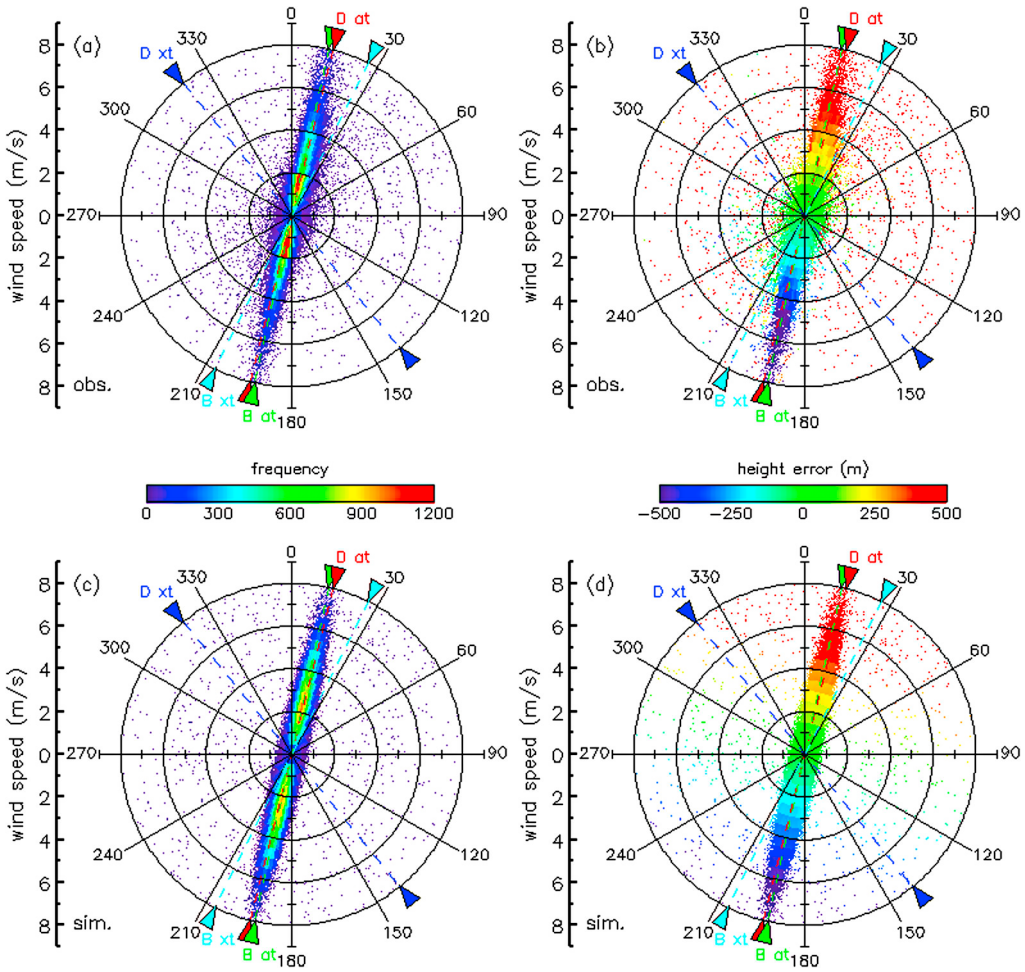

Figure 1. Distribution of observed MISR ground retrievals colored according to (a) frequency and (b) height – ground elevation difference. (c and d) The corresponding distributions of simulated ground retrievals. Triangles indicate error vector directions due to stereo matching errors in the D along-track (red), D cross-track (blue), B along-track (green), and B cross-track (cyan) positions.

CMV accuracies and usage in numerical weather prediction. The Websites of the International Winds Working Group (IWWG, http://cimss.ssec.wisc.edu/iwwg/iwwg.html) and the EUMETSAT Science Application Facility on Numerical Weather Prediction (http://www.nwpsaf.org) offer excellent and comprehensive resources on CMVs. Among other things, they provide monthly monitoring statistics against radiosonde observations and a suite of model forecasts, analysis reports on specific aspects of CMV verification, and information on how CMV data are assimilated in the major NWP centers. As examples, we present basic CMV-radiosonde comparison statistics and the main aspects of CMV usage in the ECMWF NWP model.

[22] Verifications against radiosonde observations show a CMV slow bias in most seasons and geographic areas, and at all elevations. Differences tend to be somewhat larger in the winter than summer hemisphere, especially for higher-level winds. For the low-level visible CMVs, characteristic values of bias, mean vector difference, and rmsd are 0–1 m s^{-1}, 3–4 m s^{-1}, and 3–4 m s^{-1}, respectively. For infrared CMVs, the bias at low, mid, and high level is typically 0–1 m s^{-1}, 1–3 m s^{-1}, and 1–2 m s^{-1}. The mean vector difference increases with height: 3–4 m s^{-1} at low level, 4–7 m s^{-1} at mid level, and 5–8 m s^{-1} at high level. The rmsd also increases with height: 3–5 m s^{-1} at low level, 4–8 m s^{-1} at mid level, and 6–9 m s^{-1} at high level. However, because the mean wind speed increases with height too, the normalized rmsd tends to decrease with elevation, from 0.4 to 0.5 at low level to 0.2–0.3 at high level.

[23] The ECMWF NWP system only assimilates Meteosat-9 CMVs with a QI without first guess $\geq$ 0.85. In addition, certain CMVs in specific geographic areas are blacklisted (discarded). The blacklist includes: (i) all visible winds at 700 hPa and above, (ii) all winds over land below 500 hPa, (iii) all winds over land east of 20°W and north of 20°N, (iv) all winds over land west of 20°W and north of 35°N, (v) all infrared winds below 250 hPa in the tropics (25°N–25°S), (vi) all infrared winds between 460 hPa and 700 hPa in the extra-tropics (polewards of 25°N/S), and (vii) all winds below 1000 hPa or above 10 hPa or with a view zenith angle > 60°. The CMVs also undergo variational quality control and a background check, which can apply additional penalty to winds depending on their departure from a short-term forecast from the previous model run.

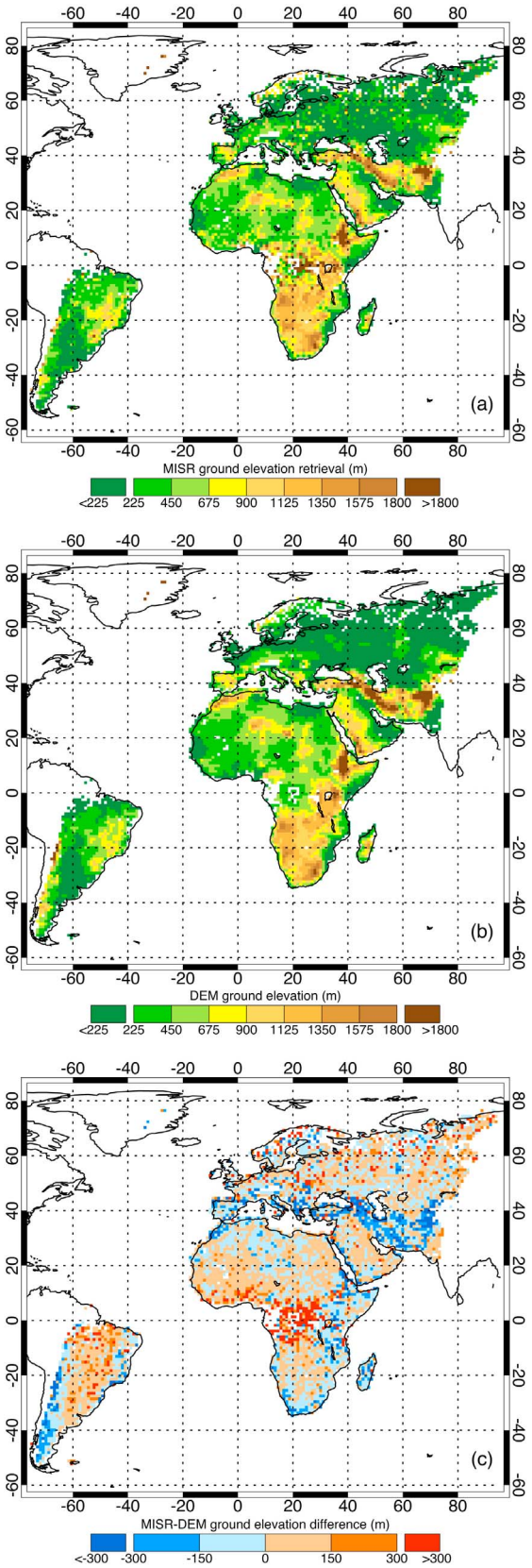

Figure 2. Mean 1° × 1° ground elevation from (a) MISR ground retrievals and (b) the digital elevation model (DEM) in the Ancillary Geographic Product, and (c) MISR-DEM ground elevation difference.

Next, winds are thinned to a lower resolution, keeping only the single highest-QI CMV in a 200 km × 200 km (horizontal) × 50–175 hPa (vertical) box. This step is required because the current assimilation system cannot account for correlated errors between neighboring retrievals. Finally, CMVs are assigned an observation error that increases with height: 2.0 m s^{-1} for low-level winds, 2.0–4.3 m s^{-1} for mid-level winds, and 4.3–5.7 m s^{-1} for high-level winds.

2.4. Comparison Method

[24] We used MISR data from the entire year of 2008, considering paths 150–230 within the Meteosat-9 coverage area. Only well-registered MISR orbits (Orbit_QA = Orbit_qa_winds = 0) were included, resulting in ∼1,500 orbits total or ∼140 orbits per month (except December and October 2008, which had only ∼70 orbits). Our final analysis used high-quality SMVs and CMVs (MISR WindQuality = 3 or 4 and CloudMotionSource ≥ 3, and Meteosat-9 QI without first guess ≥ 0.8); however, in section 4.1 we will discuss the general dependence of the wind comparison on quality flags. MISR SMVs were extracted from the Level 2 TC_STEREO product version F08_0017, while Meteosat-9 CMVs were from the MSGAMVE atmospheric motion vector data set. (MISR SMVs have recently been distributed in a Level 3 product as well, which organizes Level 2 retrievals in monthly, seasonal, and annual NetCDF files that are neither gridded nor averaged [*Mueller et al.*, 2010]. Although this new data set contains a ground filter and refined quality indicators, we favored the more mature standard L2TC product in our study.)

[25] In order to achieve the best possible temporal agreement between wind pairs, SMVs were matched with intermediate CMVs. The horizontal and temporal collocation criteria were ≤0.5° (lat/lon) and ≤15 min, respectively, well exceeding the 150 km and 1.5 h collocation thresholds recommended by the Coordination Group for Meteorological Satellites (CGMS) [*Velden and Holmlund*, 1998]. Due to the large number of Meteosat-9 retrievals, these criteria could yield multiple CMVs within the collocation window around an SMV. To find a unique match, we simply selected the CMV closest to the SMV height without imposing the ≤25-hPa CGMS constraint on vertical separation. This choice was motivated by potentially large errors in CMV height assignment and allowed us to identify areas where improvements might be necessary. The CMV pressure heights were converted to SMV geometric heights using ERA-Interim geopotential height analysis [*Dee et al.*, 2011].

3. MISR Ground Retrievals

[26] As discussed in section 2.1, MISR does not employ a priori cloud target selection and attempts retrievals in cloud-free land scenes as well. The historical reasons for this choice are twofold. First, there was no reliable cloud mask over land in the early stages of the mission. Second, ground retrievals enabled the identification and correction of gross co-registration errors, by analyzing their deviations from the near-zero wind speeds and height of topography expected in case of accurate image navigation [*Moroney et al.*, 2002].

[27] Such practical benefits notwithstanding, ground retrievals should be excluded from validation studies and data assimilation. Unfortunately, ground retrievals were not flagged in the current MISR product; thus, a scheme had to

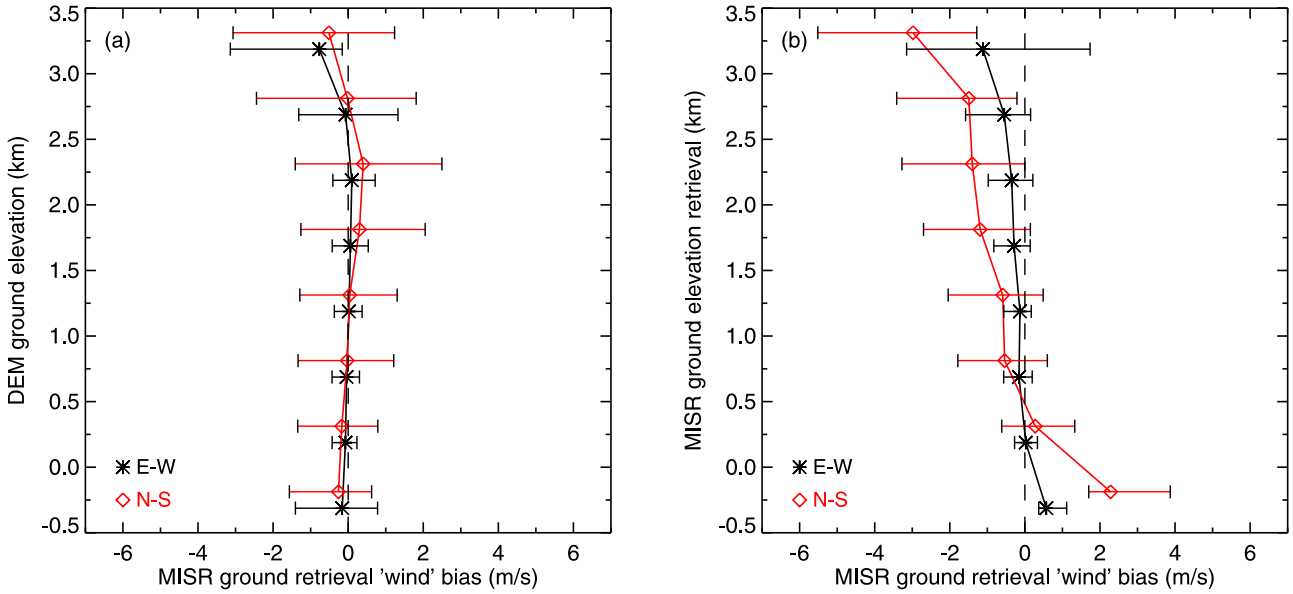

Figure 3. Vertical variation of MISR ground retrieval 'wind' bias as a function of (a) true DEM ground elevation and (b) MISR-retrieved ground elevation. Horizontal bars indicate standard deviations, separately for 'winds' larger/smaller than the bin mean. (Note that the black curve is shifted slightly downward and the red curve is shifted slightly upward for visual clarity.)

be devised to identify them in post processing. Because the locations of pixels actually tracked by the stereo matcher were not included in the TC_STEREO file, a perfectly unambiguous classification of SMVs (cloud versus ground) was not possible. However, we managed to derive an adequate scheme by analyzing the speed, direction, and height-topography difference of likely ground retrievals.

[28] In order to be as conservative as possible, we selected completely cloud-free land scenes as indicated by the nadir Radiometric Camera-by-camera Cloud Mask (RCCM), yielding 147,602 ground retrievals. Figure 1a shows the frequency distribution of these ground retrievals in a wind rose plot. The vast majority of wind speeds were small with ~80% being ≤2 m s^{-1}. The mean E-W and N-S wind components were −0.06 m s^{-1} and −0.13 m s^{-1}, respectively, indicating unbiased retrievals. In accordance with previous studies, the N-S wind showed significantly larger scatter than the E-W wind with respective standard deviations of 1.95 m s^{-1} and 0.70 m s^{-1}.

[29] The strong correlation between N-S wind error and height error is depicted in Figure 1b, colored according to the difference between retrieved height and ground elevation. Overestimation of the northerly/southerly wind component introduced a positive/negative height error, the magnitude of which clearly increased with wind speed. Regression yielded a sensitivity of −82 m height error per 1 m s^{-1} N-S wind error. In contrast, the relationship between E-W wind error and height error was rather weak, highlighting that the main challenge of MISR retrievals lies in unscrambling cloud motion and height effects in the N-S (along-track) direction. Reflecting the small N-S wind bias, the height bias was only 11 m with a standard deviation of 331 m. Overall, these results confirmed the accurate co-registration of MISR imagery and established minimum error bars for SMVs in good agreement with prelaunch estimates [*Horváth and Davies*, 2001a].

[30] To further demonstrate the quality of ground observations, we compared the retrieved mean surface elevation of 1° × 1° areas with the independent digital elevation model (DEM) in the MISR Ancillary Geographic Product (AGP), as shown in Figure 2. Although retrievals were somewhat noisier than the AGP DEM, the agreement between the height data was excellent with 75% of differences being ≤150 m and 89% being ≤300 m. (For the derivation and accuracy of the AGP DEM see *Lewicki and Zong* [1999, and references therein].) In general, MISR mean surface heights were underestimates in high narrow mountain ranges and overestimates in lower-lying areas. The largest (>300 m) positive biases in the Congo Basin were an artifact of MISR picking up biomass-burning smoke, which in turn was a consequence of the cloud mask being designed to classify smoke-covered regions as 'clear' (cloud-free) for aerosol retrievals.

[31] A peculiar feature of ground retrievals was that they were not random, but strongly favored directions 0°–30° and 180°–210°, in particular the 14°/194° direction. These angles essentially corresponded to the North-relative heading of the Terra satellite and were well captured by retrieval sensitivities to tracking location errors described by *Davies et al.* [2007, Tables 2 and 3]. For example, a ±1-pixel along-track (N-S) error in the D camera feature location introduces a cross-track and along-track wind component error of ±1.4 m s^{-1} and ±5.6 m s^{-1}, respectively, corresponding to directions 14°/194°. A similar error in the B camera along-track feature location yields cross-track and along-track wind errors of ∓3.4 m s^{-1} and ∓15.5 m s^{-1}, respectively, corresponding to directions 12°/192°. Cross-track location errors in the D and B cameras result in wind

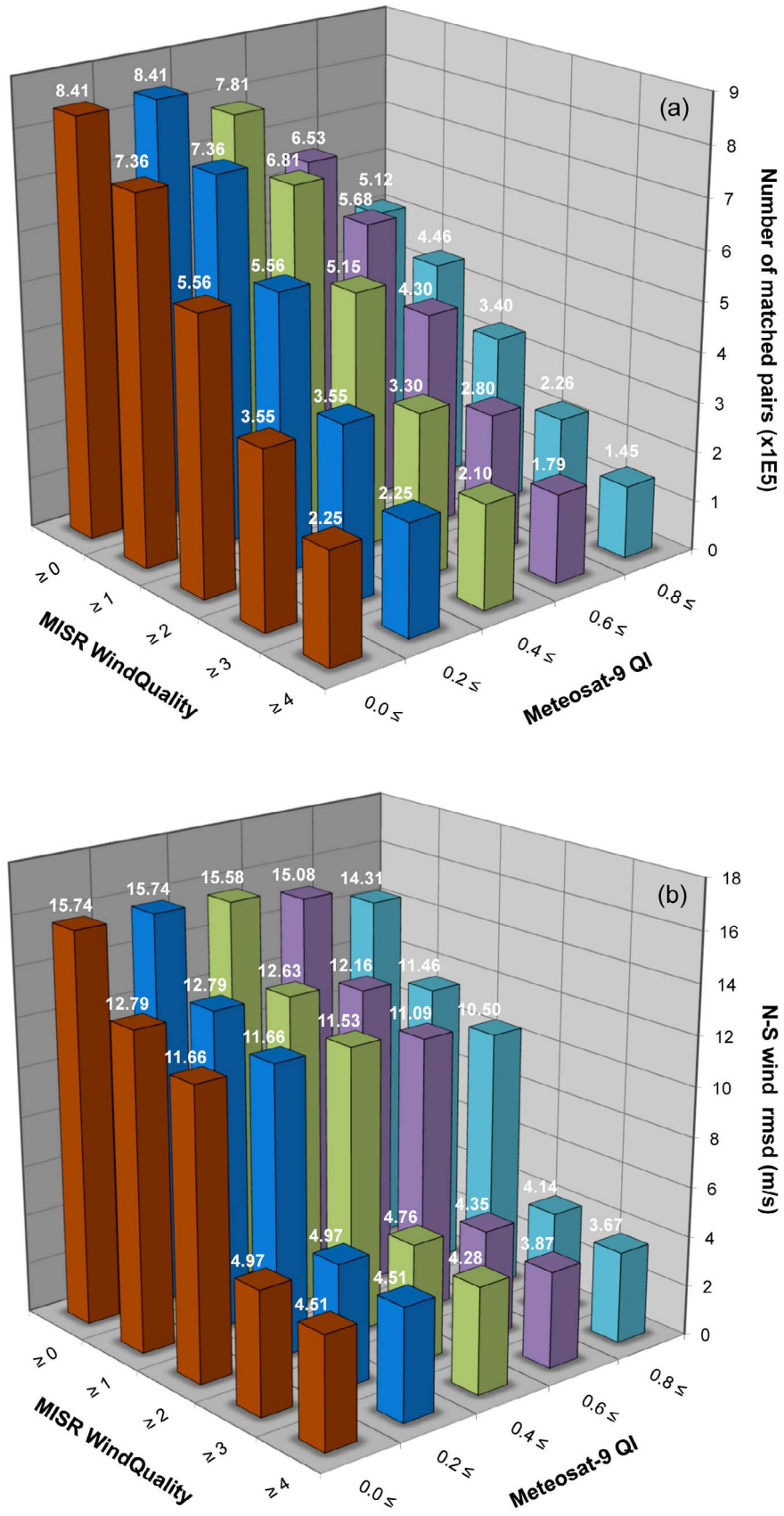

Figure 4. Dependence of SMV–CMV comparison on quality indicators: (a) number of matched pairs and (b) rmsd of north-south wind components.

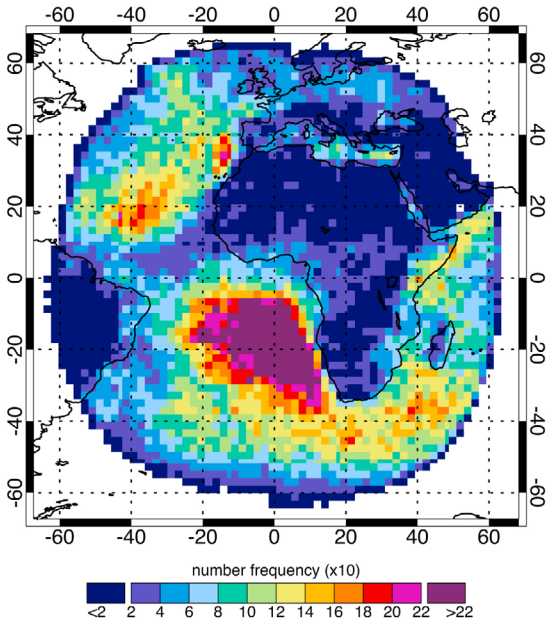

Figure 5. Geographic frequency distribution of high-quality (WQ ≥ 3 and QI ≥ 80) SMV-CMV pairs.

error vectors along the 141°/321° and 27°/207° directions, respectively, but with significantly smaller magnitudes.

[32] From the results of [*Muller et al.* 2002, Figure 2], we derived a first-order error model for the Nested Maxima matcher, which explained the observed ground retrievals fairly well when combined with the above retrieval sensitivities. Stereo matcher error distributions were approximated as the sum of a Gaussian peak centered on zero and a uniform distribution representing gross errors. We further assumed uncorrelated errors that were generally larger in the D than B camera and in the along-track than cross-track direction. Accordingly, we set the standard deviation of the central Gaussian peak in the D camera along-track and cross-track directions to 3 pixels and 2 pixels, respectively, and to 1 pixel for the B camera in both directions. Gross errors were uniformly distributed over the ± 10 pixel range in both directions with a probability of 5%.

[33] The corresponding distribution of 147,602 simulated ground retrievals is shown in Figures 1c and 1d. The observed pattern was mainly due to D camera matching errors, with the along-track and cross-track location uncertainties being responsible for the dominant 14°/194° vector direction and the spread around it, respectively. Retrievals sprinkled uniformly in all other directions were caused by gross errors. Although our model described observations fairly well, simulated vectors tended to peak at somewhat larger speeds than actual retrievals. This model shortcoming might have been due to (i) a faster-than-Gaussian drop or (ii) D/B camera and/or along-track/cross-track correlations in actual matching errors. Capturing such subtle details of ground retrievals was beyond the scope of our work and would have required a more complete picture of stereo matcher errors than the one given by *Muller et al.* [2002].

[34] We further analyzed MISR wind biases separately as a function of the true DEM ground elevation and the MISR-retrieved ground elevation. As shown in Figure 3a, when binned according to DEM ground elevation both wind components showed small biases and little vertical variation. Binning according to retrieved ground elevation, however, rearranged data such that the lowest bins were dominated by positive N-S wind biases (negative height errors), while

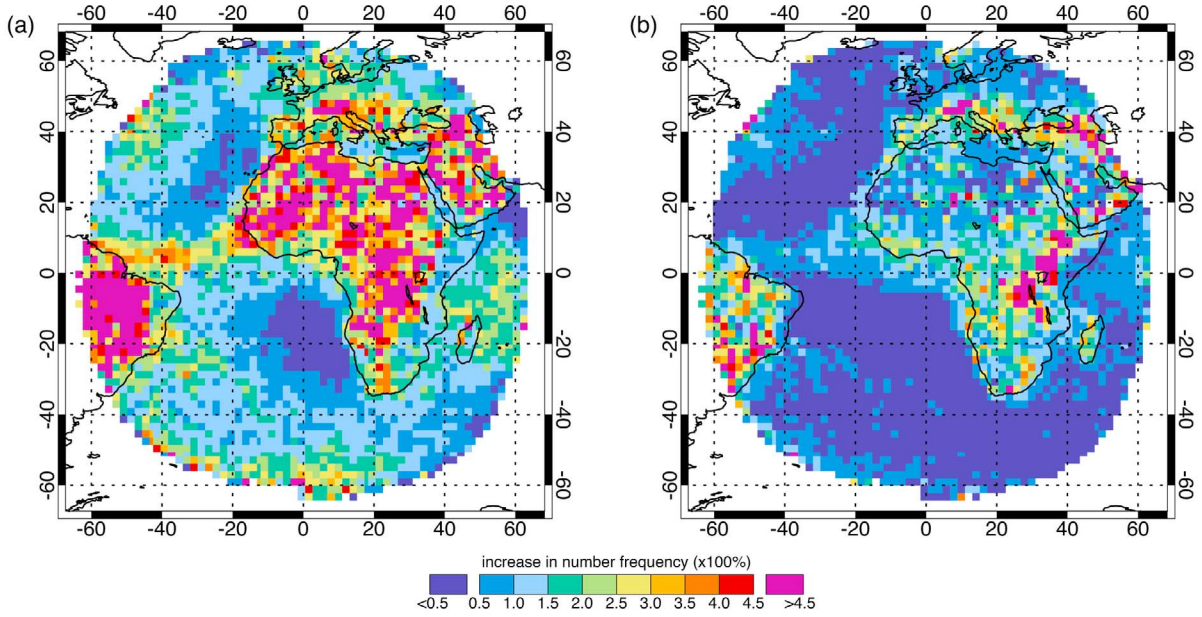

Figure 6. Geographic distribution of SMV-CMV number frequency increase due to relaxing (a) MISR quality (*WQ* ≥ *0* and QI ≥ 80) or (b) Meteosat-9 quality (*QI* ≥ *0* and WQ ≥ 3), relative to the frequency of high-quality pairs (WQ ≥ 3 and QI ≥ 80) in Figure 5. This plot essentially highlights those areas where wind retrievals most often failed our quality requirements.

Table 1. Full-Disk Annual-Mean Comparison of MISR SMVs (WQ ≥ 3) and Meteosat-9 CMVs (QI ≥ 0.8) for Low-Level (>700 hPa) Clouds, as Determined by MISR SMV Height[a]

Variable	Surface	Mean Difference	RMSD	Correlation
East-West Wind	All	−0.37 m s^{-1}	2.38 m s^{-1}	0.96
	Ocean	−0.35 m s^{-1}	2.29 m s^{-1}	0.96
	Land	−0.65 m s^{-1}	3.44 m s^{-1}	0.85
North-South Wind	All	−0.82 m s^{-1}	3.51 m s^{-1}	0.85
	Ocean	−0.83 m s^{-1}	3.49 m s^{-1}	0.85
	Land	−0.74 m s^{-1}	3.81 m s^{-1}	0.77
Wind Speed	All	0.09 m s^{-1}	2.76 m s^{-1}	0.83
	Ocean	0.13 m s^{-1}	2.68 m s^{-1}	0.84
	Land	−0.50 m s^{-1}	3.64 m s^{-1}	0.61
Wind Direction	All	−3.6°	44.1°	0.89
	Ocean	−3.1°	41.2°	0.90
	Land	−9.4°	72.4°	0.75
Height	All	439 m / −49 mb	1063 m / 93 mb	0.34 / 0.43
	Ocean	456 m / −51 mb	1023 m / 92 mb	0.32 / 0.41
	Land	205 m / −28 mb	1503 m / 113 mb	0.20 / 0.27

[a]The total/ocean/land sample number is 200,239/186,406/13,833. The mean vector difference for all/ocean/land samples is 3.00/2.96/3.56 m s^{-1}.

higher-level bins were dominated by increasingly negative N-S wind biases (positive height errors), as depicted in Figure 3b. This vertical rearrangement was the consequence of the negative correlation between MISR N-S wind error and height error, and had a direct relevance to the SMV-CMV comparison, which showed similar vertical profiles of mean differences (see section 4.5 and Figure 11).

[35] Based on the above results, MISR SMVs were excluded from further analysis as potential ground retrievals if: (i) wind speed was ≤2 m s^{-1} in directions 330°–30° or 150°–240° or (ii) wind speed was ≤4 m s^{-1} in directions 0°–30° or 180°–210° and, in addition, the nadir RCCM cloud fraction was ≤5% and height minus ground elevation difference was ≤600 m. This ground filter removed the majority of obvious outliers from the MISR – Meteosat-9 wind scatterplots without eliminating a large number of valid matches. In fact, a mere ∼0.5% of all wind pairs were flagged as 'MISR ground'; hence, their exclusion/inclusion would not have affected the overall statistics in any case.

[36] We note that *Hinkelman et al.* [2009] and the new Level 3 MISR stereo motion vector product [*Mueller et al.*, 2010] also employed ad hoc methods to screen ground retrievals. Although differing in detail, these filters follow the same basic logic, that is, retrievals with small wind speeds and heights close to the terrain elevation are unlikely to be associated with advecting clouds. In our experience, all three different post-processing ground filters produce adequate and comparable results; nevertheless, a priori cloud target selection would ultimately be more desirable.

4. Comparison Results

4.1. Dependence on Quality Indicators

[37] Our final analysis included only high-quality SMVs and CMVs. Here, we discuss the general dependence of the comparison on quality indicators. An example is shown in Figure 4, plotting the number of matched wind pairs (Figure 4a) and the root-mean square difference (rmsd) in the N-S wind component (Figure 4b) as a function of MISR WindQuality flag and Meteosat-9 QI. The rmsd dropped by a factor of 4, from 15.7 m s^{-1} to 3.7 m s^{-1}, going from none to the tightest quality control. However, this improvement came at the price of greatly reduced coverage with the number of wind pairs decreasing by almost a factor of 6. The results were apparently more sensitive to MISR WQ than Meteosat-9 QI, indicating the stereo method was more prone to blunders. In particular, the most significant improvement occurred between MISR WQ = 2 ('undetermined') and WQ = 3 ('good'), the latter representing the threshold for usable SMVs. Quality control introduced similar improvements in the E-W wind rmsd, as well as in other metrics such as mean difference and correlation. Because limiting the comparison to the highest quality MISR retrievals with WQ = 4 improved the results only marginally but reduced sampling significantly, we relaxed the MISR quality threshold to WQ ≥ 3 ('good' or 'very good') but kept Meteosat-9 QI ≥ 0.8 in the final analysis.

[38] The geographic distribution of such high-quality SMV-CMV pairs is shown in Figure 5. The largest number of wind pairs was found in stratus clouds of the Southern Oceans as well as in low-level marine stratocumulus and trade wind cumulus off the west coast of Africa and Europe, particularly in the stratocumulus region off Namibia. As noted before, the number of retrievals was vastly reduced over land, which was not surprising in dry desert regions. Over Brazil and the oceanic ITCZ, however, the low number of high-quality matches was more indicative of retrieval difficulties in convective clouds than of low cloudiness. The reduced number and quality of Meteosat-9 CMVs due to limb view geometry at the edge of the SEVIRI full disk was also evident. In addition, we noted a peculiar contrast between the western and eastern Mediterranean with the latter featuring considerably more wind pairs than the former.

[39] To investigate the role of quality control in the emergence of the above spatial distribution pattern, we calculated the relative frequency increase that resulted from relaxing either the MISR or the Meteosat-9 quality threshold, shown in Figure 6. The considerably larger effect of MISR QC on the results was apparent here too. For both instruments, land retrievals were more uncertain than oceanic ones. However, MISR QC showed a sharper land-ocean contrast and less spatial uniformity than Meteosat-9 QC. Overall, high-quality MISR SMVs were most frequently found in marine stratocumulus regions.

Table 2. Full-Disk Annual-Mean Comparison of MISR SMVs (WQ ≥ 3) and Meteosat-9 CMVs (QI ≥ 0.8) for Mid-Level (700–400 hPa) Clouds, as Determined by MISR SMV Height[a]

Variable	Surface	Mean Difference	RMSD	Correlation
East-West Wind	All	−0.99 m s^{-1}	3.76 m s^{-1}	0.96
	Ocean	−1.24 m s^{-1}	4.45 m s^{-1}	0.95
	Land	−0.76 m s^{-1}	3.00 m s^{-1}	0.95
North-South Wind	All	−2.95 m s^{-1}	6.92 m s^{-1}	0.74
	Ocean	−3.77 m s^{-1}	8.32 m s^{-1}	0.74
	Land	−2.21 m s^{-1}	5.34 m s^{-1}	0.74
Wind Speed	All	0.78 m s^{-1}	5.39 m s^{-1}	0.81
	Ocean	0.76 m s^{-1}	6.48 m s^{-1}	0.78
	Land	0.81 m s^{-1}	4.15 m s^{-1}	0.77
Wind Direction	All	−4.6°	56.1°	0.86
	Ocean	−0.9°	49.4°	0.89
	Land	−7.9°	61.6°	0.83
Height	All	274 m / −38 mb	2023 m / 148 mb	0.65 / 0.67
	Ocean	182 m / −35 mb	2053 m / 155 mb	0.69 / 0.70
	Land	357 m / −41 mb	1995 m / 141 mb	0.61 / 0.64

[a]The total/ocean/land sample number is 13,936/6,628/7,308. The mean vector difference for all/ocean/land samples is 5.42/6.52/4.43 m s^{-1}.

[40] Both wind retrieval techniques appeared more uncertain in convective clouds over Brazil and the oceanic ITCZ, which might have reflected generally larger tracking errors in fuzzy and featureless anvil cirrus. For MISR, neglecting rapid vertical development or pattern matching difficulties between the most oblique (cloud side) view and the nadir (cloud top) view were additional sources of error in such convective systems. Multilayer clouds can introduce similar tracking difficulties, which might partly explain the large number of lower quality MISR retrievals in the northwest and southernmost Atlantic and the Indian Ocean. MISR SMVs were also frequently of low quality in the Sahara and Arabian Peninsula, likely corresponding to convective or cirrus clouds. Finally, we note again the apparent contrast in the Mediterranean, where wind retrievals, especially SMVs, tended to be more uncertain in the western than eastern basin.

4.2. Full-Disk Mean Comparison

[41] The full-disk annual-mean comparison of MISR SMVs and Meteosat-9 CMVs was made separately for low- (>700 hPa), mid- (700–400 hPa), and high-level (<400 hPa) clouds. The comparison statistics somewhat depended on whether SMV or CMV heights were used for classification. The reason for this was obvious from the scatterplots in Figure 9: the MISR and Meteosat-9 low, mid, and high cloud bins did not contain exactly the same data, because wind pairs with large height differences fell into different height categories. These data clusters far off the 1:1 line will be further analyzed in section 4.4. Here, Tables 1, 2, and 3 summarize results binned according to SMV heights, while auxiliary material Tables S1, S2, and S3 give statistics for CMV height binning.[1]

[42] Approximately 89% of all wind pairs were found over ocean and ∼11% over land, and the data were dominated by low-level retrievals. In accordance with previous studies, the E-W wind components showed a smaller mean difference and rmsd, and higher correlation than the N-S wind components. Compared to Meteosat-9, MISR winds had weaker westerlies and southerlies (or stronger easterlies and northerlies) at all levels (that is, mean differences were negative). For the E-W wind, the magnitude of mean differences was typically <1 m s^{-1} and the rmsd ranged from 2 to 4 m s^{-1}. Interestingly, the worst agreement occurred for mid-level clouds over ocean. For the N-S wind, both the mean difference and rmsd steadily increased with height, from −1 m s^{-1} to −4.5 m s^{-1} and from 3 to 4 m s^{-1} to 9–10 m s^{-1}, respectively.

[43] We note that *Marchand et al.* [2007] and *Hinkelman et al.* [2009] also found weaker MISR westerlies and southerlies in their comparisons to radar wind profiler data. The *Hinkelman et al.* [2009] estimates of MISR – radar E-W and N-S wind mean differences for low-, mid-, and high-level clouds were −0.98 m s^{-1}, −1.06 m s^{-1}, −2.30 m s^{-1} and −0.55 m s^{-1}, −1.03 m s^{-1}, −4.47 m s^{-1}, respectively. The corresponding E-W and N-S wind rmsd were 3.34 m s^{-1}, 3.53 m s^{-1}, 5.36 m s^{-1} and 4.77 m s^{-1}, 5.12 m s^{-1}, 8.31 m s^{-1} for low, mid, and high levels. These values were comparable to our results and also showed a general increase in mean wind difference and rmsd with height, particularly for the N-S component. In sum, negative SMV-CMV wind differences were a robust feature, which we also observed in zonal means at all latitudes (Figure 7) and in regional means in most areas (Figure 8). A likely explanation was small but systematic uncertainties in MISR geolocation and co-registration. As we will show in section 4.6, there were uncorrected residual (sub-pixel) errors in image registration, which caused systematic cross-swath biases in MISR retrievals and might have also been responsible for the overwhelmingly negative MISR – Meteosat-9 wind differences.

[44] For high-level clouds the land-ocean contrast was weak, with slightly worse agreement over land than ocean. The only exception was N-S wind correlation, which was considerably smaller over land. For low-level clouds the land-ocean contrast was also relatively weak, with the largest differences occurring in the E-W wind statistics and N-S wind correlation, which showed larger disagreements over land than ocean. The land-ocean contrast was strongest and opposite for mid-level clouds, with significantly larger mean difference and rmsd over ocean than land, especially in the N-S wind component.

[1]Auxiliary materials are available in the HTML. doi:10.1029/2011JD016047.

Table 3. Full-Disk Annual-Mean Comparison of MISR SMVs (WQ ≥ 3) and Meteosat-9 CMVs (QI ≥ 0.8) for High-Level (<400 hPa) Clouds, as Determined by MISR SMV Height[a]

Variable	Surface	Mean Difference	RMSD	Correlation
East-West Wind	All	−0.67 m s^{-1}	3.54 m s^{-1}	0.98
	Ocean	−0.57 m s^{-1}	3.71 m s^{-1}	0.98
	Land	−0.89 m s^{-1}	3.15 m s^{-1}	0.98
North-South Wind	All	−4.42 m s^{-1}	9.49 m s^{-1}	0.86
	Ocean	−4.37 m s^{-1}	9.29 m s^{-1}	0.88
	Land	−4.55 m s^{-1}	9.92 m s^{-1}	0.75
Wind Speed	All	1.58 m s^{-1}	7.12 m s^{-1}	0.88
	Ocean	1.83 m s^{-1}	6.94 m s^{-1}	0.89
	Land	1.03 m s^{-1}	7.50 m s^{-1}	0.81
Wind Direction	All	0.6°	43.6°	0.89
	Ocean	1.3°	43.0°	0.88
	Land	−0.9°	44.9°	0.89
Height	All	702 m / −31 mb	1384 m / 71 mb	0.78 / 0.66
	Ocean	604 m / −27 mb	1294 m / 71 mb	0.80 / 0.65
	Land	917 m / −39 mb	1563 m / 71 mb	0.76 / 0.69

[a]The total/ocean/land sample number is 10,980/7,520/3,460. The mean vector difference for all/ocean/land samples is 7.13/7.14/7.11 m s^{-1}.

[45] When sliced according to MISR heights, the data showed larger mean SMV heights than CMV heights at all levels. Overall, the mean height difference was smallest at mid level, although the height rmsd was largest in this layer. The height correlation steadily decreased with decreasing height and was rather poor for low-level clouds, especially over land. For mid-level clouds, mean height differences might be attributed to MISR N-S wind errors alone. If the mean N-S wind component differences were wholly due to MISR errors, they would correspond to positive MISR height errors of 200–300 m in this layer (assuming a sensitivity of 82 m overestimation per 1 m s^{-1}). Such potential MISR biases were comparable in magnitude with the observed height differences. For low- and high-level clouds, however, MISR N-S wind errors alone would only explain an SMV height overestimation of ∼70 m and ∼370 m, respectively, which were significantly smaller than observed values. As we will discuss in section 4.4, there were large areas in the south Atlantic where Meteosat-9 boundary layer cloud heights were biased low, likely explaining most of the positive mean height difference in low-level winds. Similarly, a low bias in CMV heights in thin semi-transparent clouds might explain the positive mean difference in high-level winds.

[46] Binning the data by Meteosat-9 CMV heights introduced relatively small changes in the comparison statistics for the wind components (see auxiliary material Tables S1, S2, and S3). The only exception was the E-W wind in high-level clouds, which showed significantly larger mean differences and rmsd compared to SMV-height slicing. This poorer agreement was probably an artifact due to wind pairs in the C5 cluster in Figure 9, which corresponded to multilayer clouds where Meteosat-9 tracked the higher levels, while MISR tracked the lower levels. The height difference statistics, however, showed large changes. For low-level clouds, the mean SMV-CMV height difference remained positive but increased. The increase was particularly large over land, which was caused by wind pairs in the C2 cluster in Figure 9, representing a genuine low bias in EBBT CMV heights over warm surfaces (see discussion in section 4.4). For mid- and high-level clouds, on the other hand, the mean SMV-CMV height difference changed sign and became negative. This was caused by inclusion of wind pairs in the C4 and C5 clusters at mid- and high level, respectively (see Figure 9). Meteosat-9 heights were much larger than MISR heights in both clusters: in C4 due to a genuine high bias in CO_2-slicing CMV heights, while in C5 due to multilevel mismatch. As an added consequence of the inclusion of the various 'outlier' clusters, the height correlation sharply dropped in the high-level bin but moderately increased in the low-level bin.

[47] Although MISR – Meteosat-9 height differences could not be fully explained by a MISR wind bias alone, they did have a weak overall dependence on N-S wind component differences, as shown in Figure 10. Here, the distribution of SMV-CMV vector differences was plotted in a wind rose. Similar to MISR ground retrievals (see Figure 1), cloud-motion vector differences also favored the 14°/194° direction, albeit with a much larger scatter. In addition, the height differences (with the mean difference subtracted) showed the same general dependence on N-S wind differences, however, with a much-reduced correlation. In sum, although the MISR error pattern was clearly visible in the comparison, it only partly explained the observed wind discrepancies.

[48] Finally, we investigated how the comparison was affected by the choice of stereo matcher. In the 32 most data-rich MISR orbits, employing the area-based M2/M3 matcher instead of the Nested Maxima feature matcher increased the number of high-quality SMVs by ∼14% (11,054 versus 9,723); however, SMV-CMV comparison statistics were almost identical with only a marginal improvement. The main difference was in small-cloud-fraction domains, where the area-based matcher produced ground retrievals slightly more frequently than the feature matcher. These results confirmed that Nested Maxima was perfectly adequate to characterize the mean parallax field in the current 70.4 × 70.4 km^2 domains. This conclusion, however, is unlikely to hold true at smaller scales, where a reduction in the number of tracked cloud features would inevitably increase noise. Therefore, we recommend use of an area-based matcher in the next upgrade of the MISR algorithm if higher resolution wind retrievals were to be achieved.

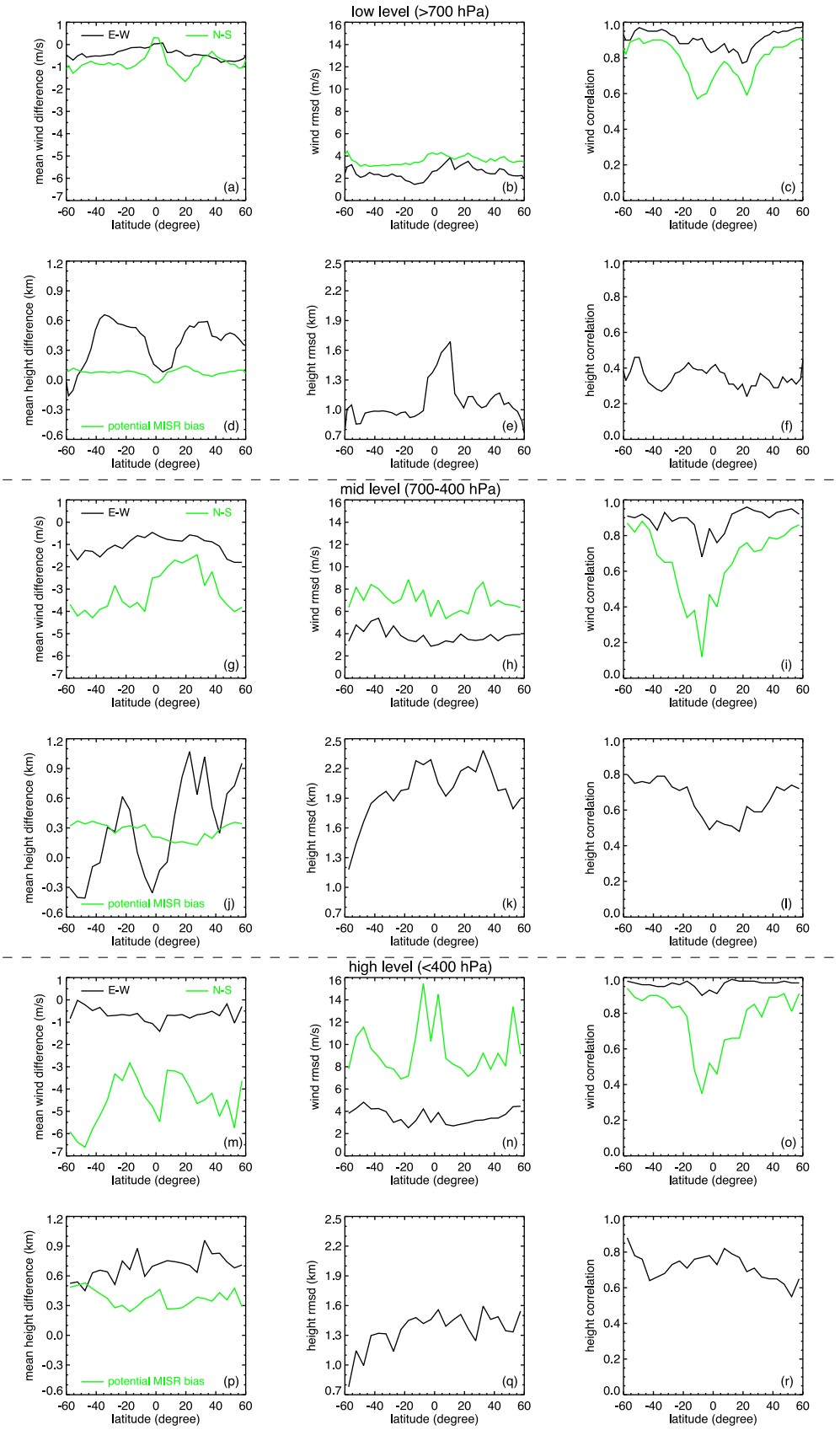
low level (>700 hPa)
mid level (700-400 hPa)
high level (<400 hPa)
E-W
N-S
mean wind difference (m/s)
wind rmsd (m/s)
wind correlation
mean height difference (km)
height rmsd (km)
height correlation
potential MISR bias
latitude (degree)
(a)
(b)
(c)
(d)
(e)
(f)
(g)
(h)
(i)
(j)
(k)
(l)
(m)
(n)
(o)
(p)
(q)
(r)

Figure 7

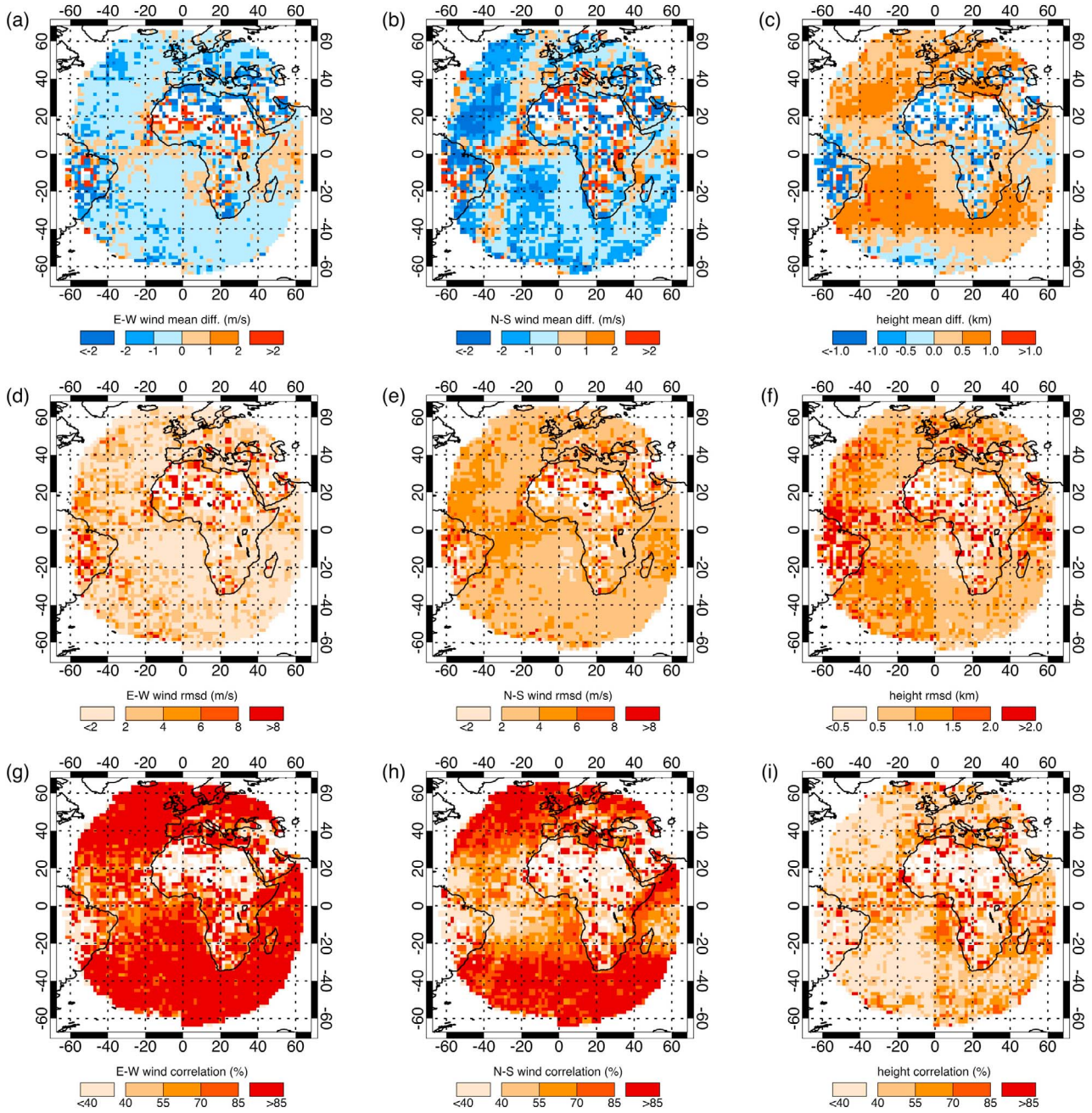

Figure 8. Geographic distribution of MISR – Meteosat-9 (a, b, and c) annual mean difference, (d, e, and f) rmsd, and (g, h, and i) correlation for E-W wind, N-S wind, and height in low-level (>700 hPa) clouds, as determined by MISR height.

4.3. Meridional Variations

[49] Meridional variations in zonal-mean comparison statistics are shown in Figure 7 for the E-W and N-S wind components, as well as height, separately for low-, mid-, and high-level clouds as determined by MISR height. Similar to full-disk-mean results, the E-W wind components showed consistently better agreement than the N-S wind components with smaller mean differences and rmsd,

Figure 7. Meridional variation of MISR – Meteosat-9 annual (a, g, and m) mean wind difference, (b, h, and n) wind rmsd, (c, i, and o) wind correlation, (d, j, and p) mean height difference, (e, k, and q) height rmsd, and (f, l, and r) height correlation, separately for low-, mid-, and high-level clouds as determined by MISR height. In Figures 7a–7c, 7g–7i, and 7m–7o, black and green correspond to the E-W and N-S wind components, respectively. In Figures 7d, 7j, and 7p, green represents the potential MISR height bias estimated from the N-S wind component difference in Figures 7a, 7g, and 7m assuming a sensitivity of −82 m per m s^{-1}.

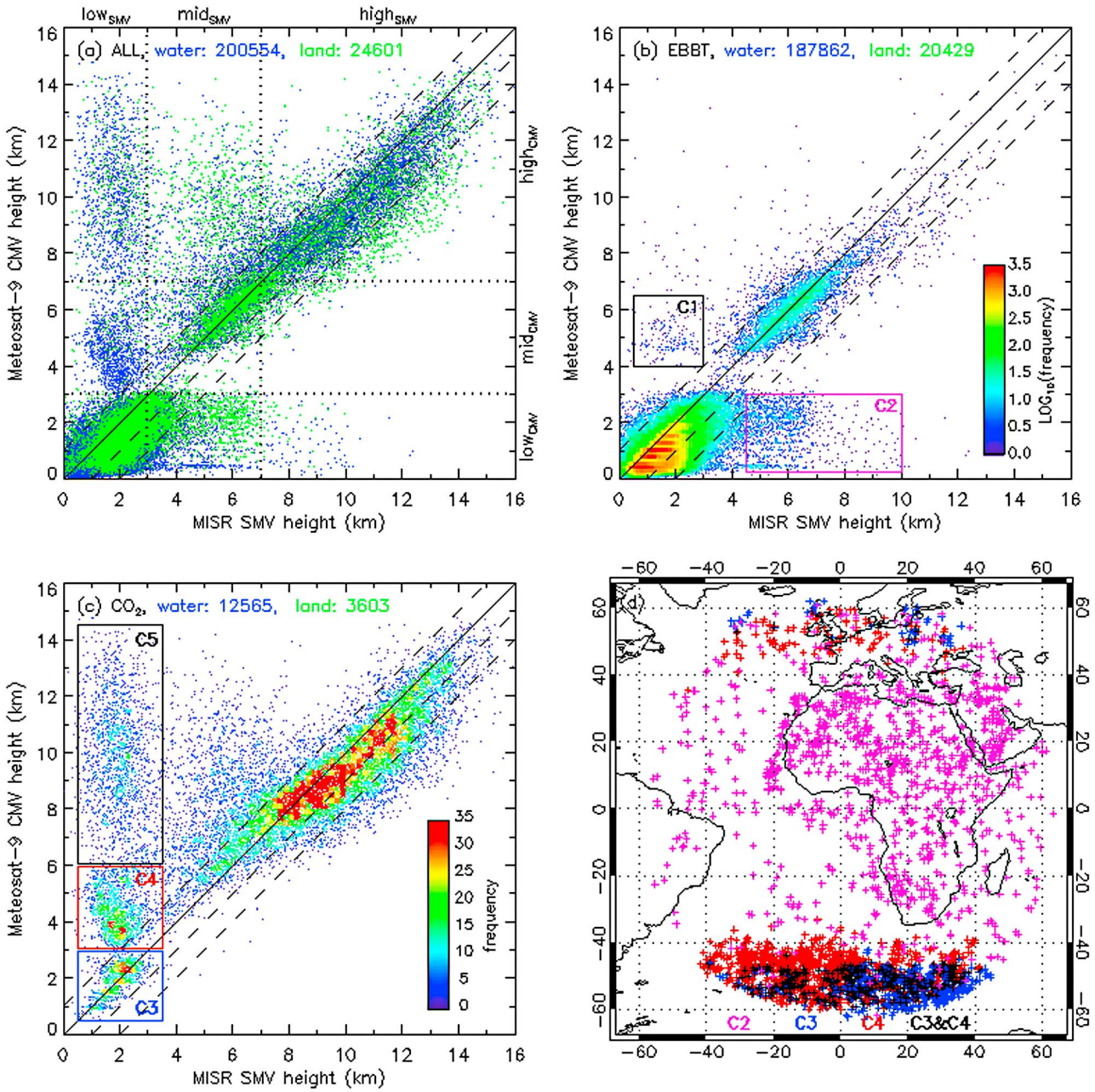

Figure 9. Comparison of MISR SMV and Meteosat-9 CMV heights for (a) all Meteosat-9 height assignment methods, (b) EBBT method, and (c) CO_2-slicing method. (d) The geographic locations of the C2, C3, and C4 cluster members from Figures 9b and 9c, colored magenta, blue, and red, respectively, with overlapping areas of C3 and C4 marked in black. In Figure 9a, blue and green correspond to water and land locations, while in Figures 9b and 9c, colors indicate number frequency. Note the different scales (logarithmic versus linear) in Figures 9b and 9c.

and higher correlations at all latitudes and levels. The MISR – Meteosat-9 mean wind differences were negative for both components at all latitudes. Mean E-W wind differences were comparable for low- and high-level clouds (0 to -1 m s^{-1}), but were noticeably larger at mid levels (-0.5 to -2 m s^{-1}). The magnitude and latitudinal variation of mean N-S wind differences, on the other hand, steadily increased with height. For low-level clouds, mean wind differences were somewhat smaller at the equator and tended to slightly increase toward higher latitudes. These smaller equatorial zonal-mean wind differences were partly due to cancellation of larger regional differences, as shown in Figure 8. While the E-W wind rmsd was comparable in all layers with only slightly larger values at mid and high levels than at low level, the N-S wind rmsd rapidly increased with height. For high-level clouds, the N-S wind rmsd was particularly large in the ITCZ and at 50°N/S but had considerably smaller values

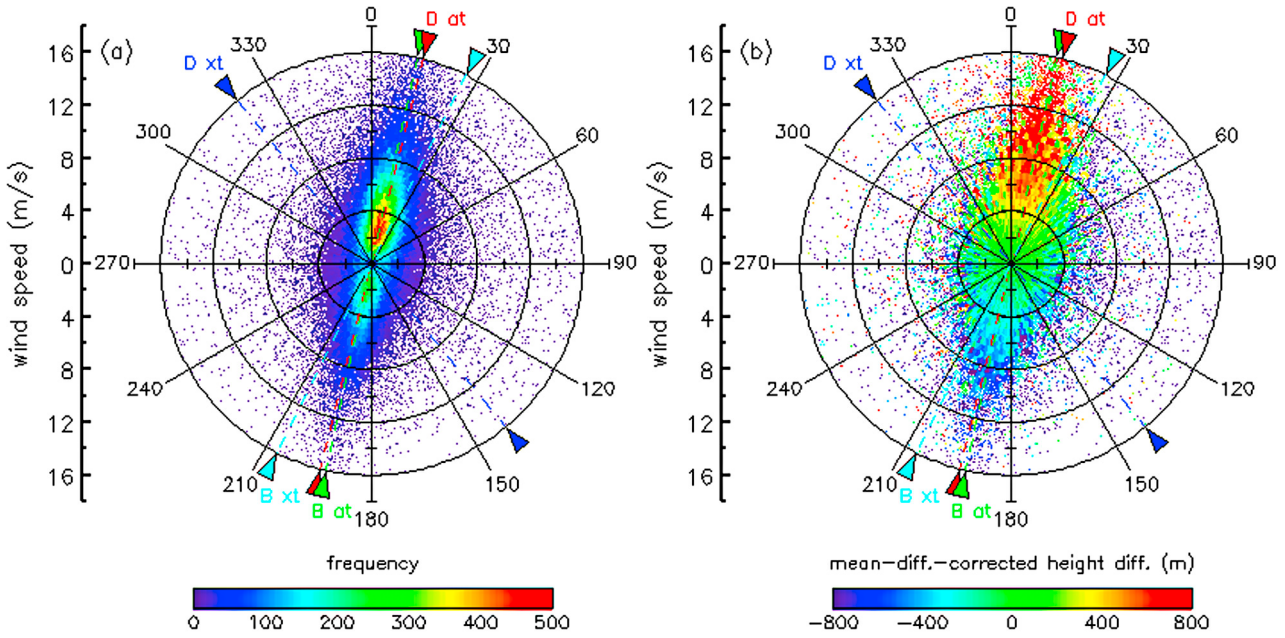

Figure 10. Distribution of MISR SMV – Meteosat-9 CMV vector difference colored according to (a) frequency and (b) mean-difference-corrected height difference (see Figure 1). Only high-quality SMVs (WQ ≥ 3) and CMVs (QI ≥ 0.8) were considered.

in the subtropics. This was mirrored by the latitudinal variation of N-S mean wind difference, which had local maxima at the equator and at 50°N/S. The large equatorial peak in high-level N-S wind rmsd was likely the result of retrieval uncertainties by both methods in the extensive thin and multilayer clouds associated with convection and, to a lesser degree, of MISR uncertainties in the vigorous but relatively small convective plumes themselves, where the neglected rapid vertical development could cause significant SMV errors.

[50] The correlation was smallest at mid levels for both wind components, particularly around the ITCZ. In general, SMV-CMV differences were the largest in this layer (at 4–5 km altitude) when data were binned by MISR SMV height. This behavior was related to the much-reduced number of mid-level geostationary winds (see Figure 11 and the accompanying discussion in section 4.5). The E-W wind correlations were largest for high-level clouds, even larger than for low-level clouds, probably reflecting the more zonal nature of the flow in the upper atmosphere. The N-S wind correlations were considerably reduced in the tropics but were reasonably good at high latitudes, in all three layers. For low-level clouds the N-S wind correlation had double minima in the subtropics (and a local maximum in between at 5–10°N), while for mid- and high-level clouds it had a single minimum at 5–10°S but with very poor values, which were probably related to convective clouds.

[51] For low-level clouds, the zonal-mean SMV-CMV height differences were positive at almost all latitudes, with the smallest values near the equator and maxima in the 20°–40° latitude bands in both hemispheres. The small mean height differences at the equator were due to cancellation of larger regional differences (see Figure 8c). The broad maxima at mid latitudes, on the other hand, were likely caused by underestimations in Meteosat-9 marine boundary layer cloud heights, as we will demonstrate in section 4.7. For mid-level clouds, the mean height difference showed the largest latitudinal variations. Height differences were larger and mostly positive in the northern hemisphere, while in the southern hemisphere both positive and negative values were encountered. Zonal-mean height differences were least variable for high-level clouds and consistently indicated SMVs 600–900 m above CMVs. This might have been caused by negatively biased CMV heights in thin semi-transparent cirrus. For comparison, we also plotted the maximum potential MISR height biases, calculated with the assumption that the N-S wind differences were exclusively due to MISR errors (see the green curves). As shown, these SMV height bias estimates were usually much smaller than the observed height differences, and the two quantities did not even correlate well.

[52] The height rmsd values were overall smallest for low-level clouds (∼1 km), somewhat larger for high-level clouds (∼1.3 km), and by far the largest for mid-level clouds (∼2 km). The height rmsd for low-level clouds showed a distinct peak between 5°S-15°N, which was mostly an artifact due to MISR tracking low clouds and Meteosat-9 tracking mid- to high-level clouds in multilayer situations (see clusters C1 and C5 in Figure 9 and the related discussion in section 4.4). Finally, the SMV-CMV height correlations sharply decreased with decreasing altitude, values being the smallest and rather poor (0.3–0.4) for low-level clouds at all latitudes.

4.4. Geographic Variations

[53] The geographic distributions of SMV-CMV mean difference, rmsd, and correlation are plotted in Figure 8 for

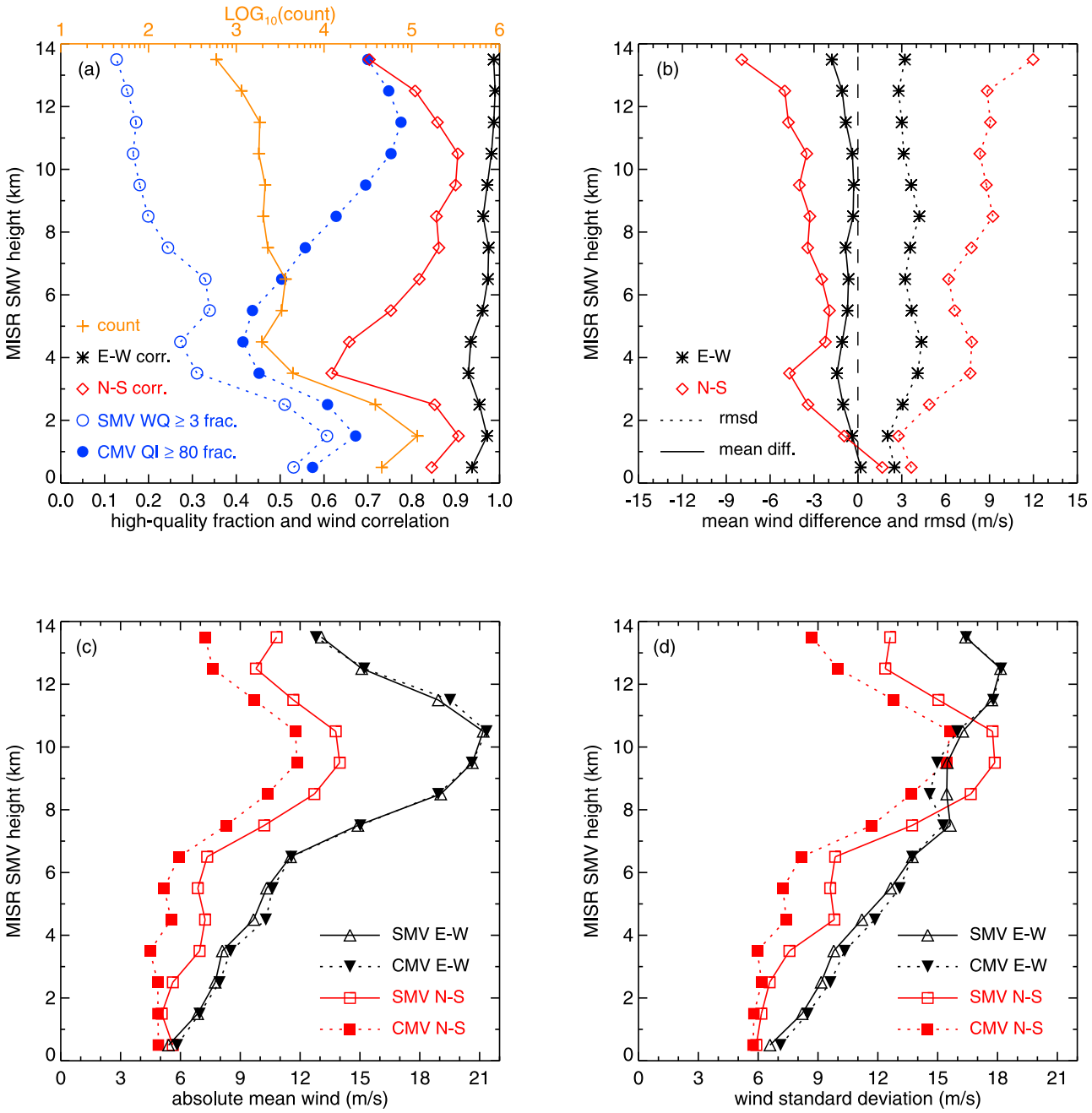

Figure 11. Height dependence of retrieval quality and the comparison statistics between high-quality SMV-CMV pairs, binned according to SMV height. (a) Open and filled blue circles correspond to the fraction of high-quality MISR SMVs (WQ ≥ 3) and that of high-quality Meteosat-9 CMVs (QI ≥ 80). Orange plus signs indicate the number of wind pairs in each height bin. Black asterisks and red diamonds show the correlation profile for the E-W and N-S components. (b) Vertical profiles of mean difference (solid lines) and rmsd (dotted lines), separately for the E-W (black asterisks) and N-S (red diamonds) components. Vertical profiles of (c) absolute mean wind and (d) wind standard deviation, separately for the E-W (black triangles) and N-S (red squares) components, and MISR (open symbols) and Meteosat-9 (filled symbols).

the E-W wind, N-S wind, and height in low-level clouds, which constitute the vast majority of our data set. Here, we used MISR height retrievals to bin data in vertical layers. Maps for mid- and high-level clouds are given in auxiliary material Figures S1 and S2, respectively, but these are statistically less significant due to the much smaller sample number.

[54] In accordance with our previous results, the agreement was significantly better for the E-W wind than the N-S wind and generally better over ocean than land. Over ocean, the mean difference was typically within ± 1 m s^{-1} for the E-W wind component and within ± 2 m s^{-1} for the N-S wind component, although meridional wind differences could be as high as 4 m s^{-1} in parts of the northern subtropical

Atlantic. The corresponding rmsd was typically ≤ 4 m s^{-1} in the E-W and ≤ 6 m s^{-1} in the N-S wind component. Larger values of N-S wind rmsd were found mostly over the Sahara and Brazil. The agreement between wind retrievals was best in marine stratocumulus off Namibia, while the largest differences occurred over Brazil, the Sahara, and the oceanic ITCZ. Also note that there were no low-level MISR winds in certain areas of the Sahara and Arabia.

[55] For both wind components, the mean difference was negative in most areas. There were only a few regions with positive mean differences: the oceanic ITCZ, the Indian Ocean, and parts of Africa for both components, the stratocumulus region off Namibia for the E-W component, and a narrow band running between continents along the full length of the Atlantic for the N-S component. This latter feature corresponded to MISR paths 207–213, which were overwhelmingly over ocean with very few land tie points. These particular paths were more often flagged by the Orbit_QA or Orbit_qa_winds flags and had generally more uncertain geolocation than other paths, affecting the more sensitive N-S wind retrieval in particular.

[56] In agreement with the full-disk-mean comparison, SMV heights were larger than CMV heights almost everywhere (Figure 8c). The largest positive differences (>0.5 km) occurred in the middle of the subtropical North Atlantic and over a large region of the South Atlantic stretching east from the Brazilian coast. There were only three areas where mean SMV heights were below mean CMV heights: Brazil, Africa (mostly the Sahara), and the very southern edge of the Atlantic, with the largest negative differences (<-1 km) occurring over Brazil. The negative SMV-CMV height differences in the very south Atlantic were related to high biases in CMV CO_2-slicing heights (see cluster C4 in Figure 9 and the corresponding discussion later in this section). The scatter between the assigned heights was generally larger over land than ocean; however, the oceanic ITCZ also featured rather high (>1.5 km) rmsd values (Figure 8f). The best overall height agreement with the smallest differences and rmsd was found in marine stratocumulus off Namibia, similar to the wind vector comparison.

[57] The correlation between the E-W wind components was generally very good, with the exception of the oceanic ITCZ, Brazil, and the Sahara (Figure 8g). The correlation between the N-S winds was smaller than that between the E-W winds everywhere, and it was particularly poor throughout the Tropics (25°S–25°N) (Figure 8h). The N-S wind correlation was also considerably poorer over land than ocean. Nevertheless, the mid- to high-latitude oceanic areas, especially the Roaring Forties and Furious Fifties in the Southern Oceans, showed good correlation (>0.85) between SMVs and CMVs even in the N-S component. Height correlations were generally rather poor, especially over land (Figure 8i). The correlations were, however, somewhat better in the eastern than western hemisphere and over the ITCZ than other parts of the Atlantic.

[58] The spatial analysis above identified a few areas where the discrepancy between SMVs and CMVs tended to be the largest. Specifically, Brazil, the oceanic ITCZ, the Indian Ocean northeast of Madagascar, and the northwest Atlantic. As discussed in section 4.1 and shown in Figure 6, these were also the areas where both wind retrievals, but MISR SMVs in particular, were often of lower quality. Likely reasons for the reduced number of high-quality stereo winds in these areas included the presence of multilayer clouds, matching difficulties between the most oblique and nadir views, and breakdown in convective clouds of the MISR assumption of no vertical cloud motion. These spatial comparison maps also suggested that the small zonal-mean differences between low-level SMVs and CMVs around the equator (5°S–10°N, Figures 7a and 7d) were partly due to cancellation of larger regional differences.

[59] The most challenging and important part of the SMV-CMV comparison is the interpretation of height differences, because the biggest potential of MISR is the more accurate stereo height assignment. A visual comparison of the N-S wind and height difference maps (Figures 8b and 8c) indicates little spatial correlation between these quantities. Even if one assumes N-S wind differences arising due entirely to MISR errors, their relatively small magnitudes would only explain SMV height overestimations of a couple of hundred meters, which are considerably smaller than the observed height differences in most areas. In addition, over Brazil, Africa, and the southernmost Atlantic the mostly negative N-S wind differences would suggest positive SMV-CMV height differences, contrary to observations. Therefore, other factors must have been at play as well.

[60] The comparison maps for mid- and high-level clouds are considerably noisier than those for low-level clouds because of poorer sampling (see auxiliary material Figures S1 and S2). They show more pronouncedly negative mean differences in both the E-W and N-S wind components. The regional mean SMV-CMV height differences were generally larger than for low-level clouds. For upper-level clouds the height differences were overwhelmingly positive, that is, MISR heights were larger than CMV heights almost everywhere. This might have been related to low biases in CMV heights in thin semi-transparent cirrus. For mid-level clouds, however, both negative and positive mean height differences were found. Cancellation of these larger regional means would explain that the full-disk mean height difference was smallest at mid level (see Table 2).

[61] The E-W wind rmsd values were only slightly larger for mid- and high-level clouds than for low-level clouds. However, the N-S wind rmsd steadily increased with height in most areas. The height rmsd was somewhat larger for high-level clouds than low-level clouds, especially over Africa. Mid-level height rmsd values, on the other hand, were markedly larger everywhere than their low-level counterparts. The E-W wind correlations were generally comparable in all three layers, but over Brazil and the oceanic ITCZ the values were somewhat larger at mid- and high-level than at low level. Regional N-S wind correlations were also quite comparable in all layers, except maybe the Tropical oceans where they tended to be the lowest at mid levels. The most dramatic vertical differences were observed in height correlations, which were far better for mid-level and especially high-level clouds than for low-level clouds in most regions. Finally, mid- and high-level MISR SMVs did occur in the Sahara and Arabia, where low-level SMVs were often completely missing. However, there were no mid- and high-level SMVs in the middle of the tropical South Atlantic.

[62] In order to gain a better understanding of the above height differences, we analyzed the scatterplot of SMV and

Table 4. Comparison of MISR SMVs and Meteosat-9 CMVs for the Clusters in Figure 9

Variable	C1	C2 Ocean / Land	C3	C4	C5
MVD[a]	8.87 m s^{-1}	11.11 / 4.37 m s^{-1}	3.12 m s^{-1}	4.56 m s^{-1}	18.74 m s^{-1}
NRMSVD[b]	1.15	1.07 / 0.85	0.29	0.51	2.21
Wind Speed Mean Difference	−3.05 m s^{-1}	6.42 / 1.79 m s^{-1}	−0.81 m s^{-1}	−1.87 m s^{-1}	−9.43 m s^{-1}
Wind Speed RMSD	8.05 m s^{-1}	15.91 / 8.65 m s^{-1}	2.33 m s^{-1}	5.63 m s^{-1}	15.03 m s^{-1}
Wind Direction Mean Difference	10.0°	−6.6° / −3.1°	4.4°	0.4°	−52.5°
Wind Direction RMSD	97.1°	79.1° / 55.2°	27.2°	29.2°	138.3°
Sample Number	173	473 / 800	870	1348	1527

[a]Mean vector difference.
[b]Root mean square vector difference normalized by MISR wind speed.

CMV heights, given in Figure 9a separately for ocean (blue) and land (green). The visually most striking discrepancies occurred in the data cluster where MISR heights were in the 1–3 km range but Meteosat-9 heights were vastly larger, reaching altitudes up to 14 km. Apart from this cluster, wind heights above 5 km were in significantly better agreement, closer to the 1:1 line. In the lower troposphere below 3 km, agreement was also better but MISR clearly retrieved higher altitudes than Meteosat-9. Next, we further separated wind pairs according to CMV height assignment: Figure 9b and Figure 9c correspond to the equivalent blackbody brightness temperature (EBBT) method and CO_2-slicing, respectively. (The water vapor intercept method is not shown because it represented an insignificant number of samples.) We selected five data clusters for detailed study, to determine if the observed height discrepancies represented genuine biases or were simply artifacts due to multilevel mismatches. The SMV-CMV comparison statistics for these clusters are summarized in Table 4. We visually analyzed each cloud scene in these clusters, overlaying the MISR and Meteosat-9 wind vectors on MISR imagery. The most oblique (70°) MISR Df/Da views proved particularly useful identifying thin high-level cloud and dust layers that were otherwise undetectable in the nadir view.

[63] Collocated wind pairs with CMVs using the EBBT height assignment method represented ∼93% of our data. Figure 9b shows two main concentrations of data separated by a gap in EBBT heights in the 3–4.5 km range. At mid- to high levels above 4.5 km, SMV and CMV heights were in good agreement with the majority of data points being along the 1:1 line. For the small portion of data above 8 km, however, MISR heights were clearly larger. At lower levels below 3 km, SMV heights tended to be significantly larger than CMV ones. The tendency of CMV heights to populate discrete levels was also evident; this feature was likely due to use of forecast temperature profiles provided at fixed pressure levels.

[64] The data gap between 3 and 4.5 km mostly reflected a nonlinear shift in height assignment from cloud top to cloud base at that particular level. As discussed in section 2.2, CMVs are assigned to cloud base or the NWP model inversion height, rather than cloud top, when the initial pressure is >650 hPa. A compounding factor might have been that height assignment is also more challenging in this layer, resulting in a much-reduced number of mid-level geostationary winds [*Forsythe and Doutriaux-Boucher*, 2005]. The CO_2-slicing method is less reliable and often fails at mid level due to loss of sensitivity deeper in the troposphere. The EBBT method can frequently be in error as well, if the cloud is thin or sub-pixel. Additionally, mid-level cloud is quite common in difficult multilayer situations. Therefore, the height assignment method used is more variable and the retrieved heights are less consistent at mid level, reflecting the transition from use of CO_2-slicing that dominates at higher levels to the EBBT method at lower levels. In sum, there is a shift at 3–4.5 km (∼650 hPa) in both the height retrieval method (from CO_2-slicing to EBBT) and the cloud level at which CMVs are assigned (from cloud top to cloud base).

[65] The largest concentration of data below 2.5 km mostly corresponded to scenes where SMVs and CMVs tracked the same low-level marine clouds, were in excellent agreement regarding wind speed and direction, but SMV heights were 1–2 km larger than CMV ones. A portion of these differences could certainly be attributed to MISR retrieving cloud top heights, while Meteosat-9 assigns CMVs to cloud base, where they are more representative of the flow. Assuming a typical marine stratocumulus thickness of 300 m [*Stevens*, 2005], however, would only explain an SMV height overestimation of a couple of hundred meters due to such algorithmic differences. As we will demonstrate through a case study in section 4.7, a more plausible explanation was that Meteosat-9 EBBT heights were often biased low for marine boundary layer clouds, even after considering cloud base adjustments.

[66] The analysis of the two clusters with the largest EBBT height discrepancies yielded the following results. In cluster C1, the vast majority of scenes contained multilayer clouds. The large vector/speed differences and direction rmsd confirmed our visual analysis that MISR tracked the lower layers while Meteosat-9 tracked the mid levels; hence, the large height differences were an artifact. Cluster 2 represented a wider variety of situations. As shown in Figure 9d (magenta symbols), 2/3 of the scenes in this cluster were over land (Africa and Arabian Peninsula). The SMV-CMV comparison statistics in Table 4 indicated a sharp contrast between land and ocean scenes. The relatively small wind differences over land suggested that both instruments mostly tracked the same clouds. Visual analysis indeed confirmed that most scenes were of single-layer mid- to high-level convective clouds or thin cirrus with a good agreement between wind vectors. However, CMV EBBT heights were clearly biased low due to contributions from the warm land surface. Over ocean, the significantly larger wind vector differences, in contrast, pointed to the instruments tracking clouds at different levels. Our visual analysis found most oceanic scenes in this cluster containing extensive thin cirrus or desert dust over low-level clouds. The dust

scenes were located off the North African and Arabian coasts, and were easy to identify by their brownish color. Interestingly, in these oceanic scenes MISR tracked the higher levels and Meteosat-9 tracked the lower levels. Despite the stereo technique's general preference for low clouds, it is still possible for MISR to track higher layers than Meteosat-9 if the dominating cirrus or dust completely obscures the lower layers in the oblique Df/Da views. In cluster 2, we also noticed a few CMVs with large (20–30 m s^{-1}) wind speeds assigned to levels below 1 km, which clearly indicated low biases in the EBBT heights. *Cotton and Forsythe* [2010] noted such spuriously fast low-level CMVs as well.

[67] The scatterplot of wind heights with CMVs using CO_2-slicing is shown in Figure 9c, corresponding to ~7% of our data set. The group of points identified in Figure 9a with MISR indicating low-level clouds and Meteosat-9 retrieving mid- to high-level clouds was clearly associated with the CO_2-slicing method. Height differences were the largest and visually most striking in cluster C5, but they represented a very small portion of collocated wind pairs. The vast majority of scenes in C5 were of low-level boundary layer clouds below thin cirrus, where MISR tracked the low levels and Meteosat-9 tracked the higher levels. The SMV-CMV vector/speed differences and direction rmsd were the largest for this cluster in Table 4, further confirming that the large height differences were an artifact of multilevel mismatch.

[68] The most populous data cluster in Figure 9c contained retrievals above 7 km where SMV and CMV heights were in fairly good agreement, although above 9.5 km MISR heights were ~1 km larger on average. This latter discrepancy might have been related to negative biases in CMV CO_2-slicing heights in cases of high-level semi-transparent cloud overlying lower-level cloud [*Cotton and Forsythe*, 2010]. Two additional clumps of data could be discerned at lower altitudes: clusters C3 and C4. In cluster C3, both MISR and Meteosat-9 identified low-level clouds and the corresponding heights were in very good agreement with essentially no mean difference. In cluster C4, however, Meteosat-9 indicated mid-level CMVs approximately 1.5–2 km above the low-level MISR SMVs. As shown in Figure 9d, both clusters contained winds from the same general area: the Southern Oceans poleward of 40°S; C3 sampled the eastern part a bit more, while C4 had a slight preference for the western part. Visual analysis revealed that the majority of C3 retrievals were obtained in low-level single-layer clouds, most frequently in open cell convection. Cluster C4 contained the same boundary layer cloud types as C3, but very often with thin cirrus above. The SMV-CMV wind differences were small in both clusters (see Table 4), indicating that even in the multilayer C4 scenes Meteosat-9 tracked the same low-level clouds as MISR. However, the CO_2-slicing heights assigned to these low-level CMVs were apparently biased high. *Cotton and Forsythe* [2010] also noticed the CO_2-slicing method occasionally putting low-level winds to mid level and hypothesized the presence of multiple cloud layers as a possible explanation. Our results showed that this was the case indeed.

[69] In sum, the large height differences in clusters C1 and C5 were mostly artifacts due to the instruments tracking different atmospheric layers; however, in clusters C2 and C4 they indicated genuine CMV height biases caused by radiance contributions from the warm surface (EBBT underestimation) or the presence of multiple cloud layers (CO_2-slicing overestimation). These findings also highlighted a limitation in the operational MISR and Meteosat-9 data sets: neither of them stored the image of the actually tracked cloud patterns. As a consequence, it was impossible to unambiguously filter out multilayer cases, such as the ones in clusters C1 and C5, where the two instruments retrieved cloud motion at different levels. Future studies could explore eliminating such multilevel mismatches by saving and comparing images of tracked cloud patches. In addition, more case studies in the vein of section 4.7 will be required to fully confirm and quantify the advantages of SMV stereo heights over CMV heights in clusters C2 and C4.

4.5. Vertical Variations

[70] Earlier evaluations of MISR winds already noted potential quality variations with cloud height. For example, *Davies et al.* [2007] and *Hinkelman et al.* [2009] computed difference statistics separately for low-level (<3 km or >700 hPa), mid-level (3–7 km or 400–700 hPa), and high-level (>7 km or <400 hPa) SMVs. Compared to both forecast winds and wind profiler measurements, SMVs showed larger absolute differences and rmsd at higher elevations. The RMS vector difference increased from ~5 m s^{-1} at lower levels to 8–10 m s^{-1} at higher levels, with deviations being larger in the N-S wind component than the E-W wind component. However, relative to mean wind speeds, which also increased with height, MISR retrievals were actually found to perform better at higher altitudes.

[71] Here, we investigate height dependencies in the SMV-CMV comparison at a vertical scale much finer than allowed by the coarse low-, mid-, high-level categories of previous comparisons or our own analysis in section 4.2. As noted earlier, the vertical variation of comparison statistics somewhat depends on the choice of the height used for binning (MISR versus Meteosat-9). Therefore, we performed calculations separately for SMV and CMV height binning, although we only show results for the former in Figure 11. (In general, CMV height binning produced similar vertical profiles as given in auxiliary material Figure S3, but we will discuss the main differences in this section.)

[72] Regardless of quality, the vertical distribution of MISR wind retrievals was heavily skewed toward lower elevations. The total number of SMVs dropped by ~90% between 1 km and 5 km, which was not surprising given the MISR stereo matchers' tendency to favor lower level, higher-contrast cloud targets in multilayer situations. As a compounding factor, the fraction of high-quality (WQ ≥ 3) SMVs also strongly decreased with height (see open blue circles in Figure 11a). This was most likely due to larger uncertainties in the tracking of featureless cirrus clouds with the noisy Nested Maxima matcher, especially in the most oblique D camera views. The corresponding vertical profile of the high-quality (QI ≥ 80) CMV fraction is also plotted (see filled blue circles in Figure 11a). Below 6 km, the MISR and Meteosat-9 high-quality-wind fractions showed similar vertical variations, including a local minimum between 4 and 5 km, and below 3 km they were even comparable in magnitude. Above 6 km, however, the two curves showed diverging trends as the proportion of good CMVs increased but that of good SMVs decreased with height. Differences

were most dramatic in the upper troposphere (10 km and above), where only ~15% of SMVs passed the quality test compared to ~75% of CMVs.

[73] With these results in mind, we then investigated the height dependence of the SMV-CMV comparison statistics for high-quality retrieval pairs. As shown, vertical variations in the E-W wind component were small with a mean difference below 2 m s^{-1} and rmsd of 3–4 m s^{-1} at all levels. As always, the agreement in the N-S wind component was poorer and showed significant height dependence with the mean difference and rmsd increasing from 2 m s^{-1} to 8 m s^{-1} and from 3 m s^{-1} to 12 m s^{-1}, respectively, between the near surface and 14 km altitude. As indicated in Figure 9, CMV heights below 8 km were mostly obtained by the EBBT method, while above 8 km they were retrieved almost exclusively by the CO_2-slicing method. When considering only CO_2 slicing, the SMV-CMV comparison got slightly better with height, especially above 5–6 km, indicating the height range where this method had the most skill.

[74] Apart from the lowermost layer, the SMV-CMV mean differences were negative at all levels. The correlation between the E-W wind components was greater than 0.93 at all altitudes and even increased with height, which probably reflected the stronger and predominantly zonal flow at higher elevations. The correlation between the N-S wind components was considerably smaller and showed a more complex vertical pattern with an absolute minimum of only ~0.63 in the 3–5 km height range. The SMV-CMV discrepancies were generally larger in this particular layer, as also evidenced by the local maxima in N-S wind mean difference and rmsd.

[75] As noted above, the fraction of high-quality winds dropped in this layer. The number of wind pairs per height bin (orange curve), however, showed only a slight local minimum in this general area and was not much smaller than at higher levels; hence, we ruled out insufficient sampling as the source of the larger N-S wind differences. The most likely explanation was the generally much-reduced number of CMVs, and particularly, the almost complete lack of EBBT heights in this layer (see Figure 9b). Consequently, binning by MISR height resulted in a large number of wind pairs, in which an SMV was matched with a CMV from a significantly different altitude (note: we did not constrain the maximum allowed SMV-CMV height difference in our data set). The SMV-CMV height rmsd was by far the largest (2.5 km) in this SMV altitude bin, further supporting this hypothesis. A compounding factor was the inverse correlation between MISR N-S wind error and height error, which tended to rearrange the data such that higher altitude bins preferably contained SMVs with larger negative N-S wind errors (thus, larger positive height errors).

[76] Indeed, when data were binned by CMV height (see auxiliary material Figure S3), the agreement between N-S winds at mid levels became significantly better, with increased correlation (0.85 versus 0.63) and reduced mean difference (2 m s^{-1} versus 4.5 m s^{-1}). The N-S mean wind difference in the lowermost layer also switched sign to a small negative value, indicating that the positive value obtained for SMV height binning was due to the aforementioned correlation between MISR wind and height errors (see Figure 3 in section 3). Other notable changes included slightly reduced N-S mean difference, significantly increased E-W wind rmsd, and reduced E-W wind correlation at higher altitudes.

[77] To put these mean differences in context, we plotted the vertical profiles of the absolute mean wind speeds and wind standard deviations in Figures 11c and 11d. The mean MISR/Meteosat-9 wind speed increased from 8.5/8.3 m s^{-1} to 27.2/26.0 m s^{-1} between the surface and ~11 km, with an increase in the E-W wind component from 5.4/5.8 m s^{-1} to 21.2/21.4 m s^{-1} and in the N-S wind component from 5.6/4.9 m s^{-1} to 13.8/11.8 m s^{-1}. The resulting normalized rmsd in both the E-W and N-S wind components, however, had a more complex vertical variation (not shown). Relative differences increased from the surface up to 4–5 km where they reached their maximum, reflecting the general deterioration of the comparison at this altitude. Above 5 km, normalized differences steadily decreased reaching their minimum at a height of 10–11 km, above which they increased again.

[78] The agreement between E-W winds was excellent both in terms of absolute mean and standard deviation. For N-S winds, the agreement was also good in low-level clouds below 3 km; however, in mid- and high-level clouds MISR retrieved wind speeds and standard deviations 2–4 m s^{-1} larger than Meteosat-9. Results were largely similar for Meteosat-9 height binning except that the zonal wind maximum occurred at lower altitudes (8–9 km versus 10–11 km) and CMV E-W winds were 1–2 m s^{-1} stronger than SMV E-W winds above 7 km. These profile differences probably reflected a low bias in CMV heights in thin high-level semi-transparent clouds.

4.6. MISR Cross-Swath Dependence

[79] In our analysis so far, we did not consider the effect of view geometry on our results. However, establishing the consistency, or lack thereof, of the comparison statistics with respect to geometrical factors could boost confidence in the wind retrievals, or reveal algorithmic deficiencies needing to be addressed. Due to its polar orbit, the MISR view geometry for any given camera stays the same from pole to pole. The quality of SMVs, however, can potentially vary west-to-east across an orbital swath. In the following, we summarize our findings on the significance of such MISR view dependencies.

[80] A single pole-to-pole MISR orbit is divided into 180 data blocks with each block comprising two rows of eight mesoscale (70.4 × 70.4 km^2) domains for wind retrieval. The cross-swath domain index ranges from 1 at the western edge to 8 at the eastern edge of the swath. Edge domains 1 and 8, however, were usually empty or contained inadequate amount of data for a successful retrieval and, thus, were excluded from the subsequent analysis. Before studying the cross-swath dependence of SMV-CMV differences, we first considered that of MISR ground retrievals described in section 3. Figure 12a shows E-W "wind" bias (black asterisks), N-S "wind" bias (red diamonds), and height bias (blue triangles) as a function of cross-swath location, averaged over all ground retrievals. There was a clear variation across the swath in all three quantities, with "wind" biases being the smallest and negative on the western side, increasing to larger positive values in the middle, and then decreasing to their negative maxima on the eastern side. The magnitude of variation was a relatively small 0.6 m s^{-1} in the E-W wind

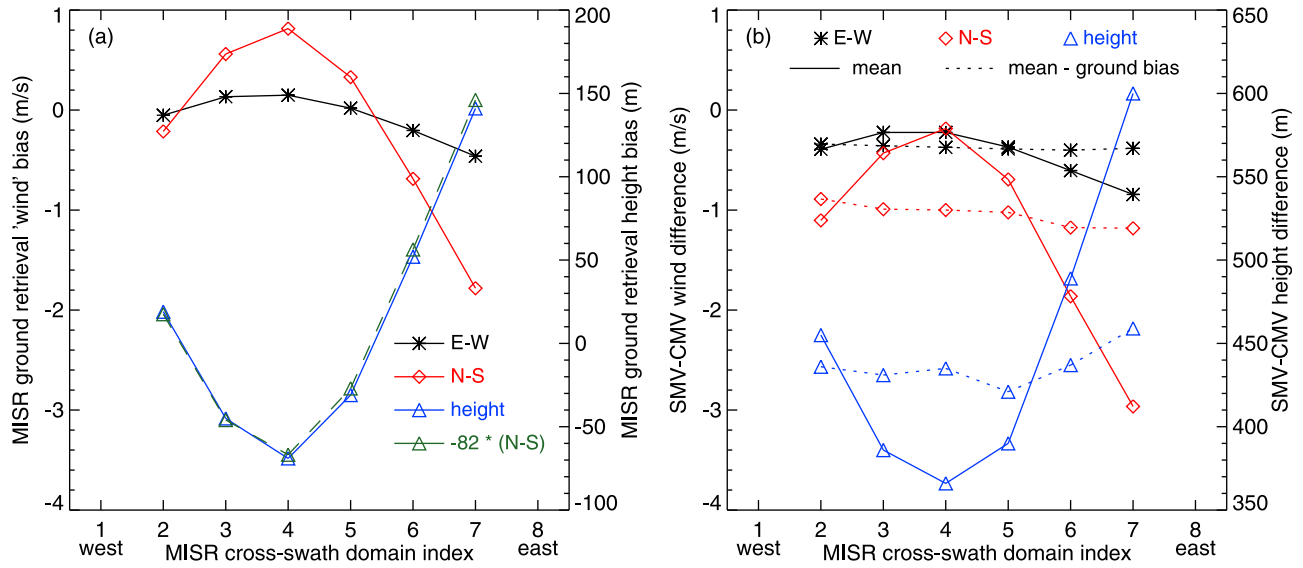

Figure 12. Cross-swath dependence of (a) MISR ground retrievals and (b) MISR SMV – Meteosat-9 CMV differences. Black asterisks, red diamonds, and blue triangles correspond to E-W wind, N-S wind, and height. In Figure 12a, green triangles depict the height bias estimated from the N-S wind bias assuming an −82 m per m s^{-1} sensitivity. In Figure 12b, solid lines show the observed mean differences, while dotted lines refer to residual differences after subtracting the corresponding ground biases in Figure 12a from the observed mean differences.

component; however, it was a considerable 2.6 m s^{-1} in the N-S wind component. The cross-swath variation of height bias had an amplitude of 210 m and mirrored that of the N-S wind bias due to the strong coupling between these two parameters. This coupling was demonstrated by the excellent agreement between the observed height bias (blue triangles) and the bias estimated with the previously derived −82 m per m s^{-1} height error sensitivity to N-S wind error (green triangles).

[81] The cross-swath dependencies of mean SMV-CMV differences plotted by the solid lines in Figure 12b were very similar to those of ground retrieval biases, indicating an algorithm deficiency affecting MISR retrievals in general. The mean Meteosat-9 wind components and height, on the other hand, exhibited remarkable consistency when binned according to MISR cross-swath location. (SMV-CMV correlation and rmsd were also quite consistent across the swath.) As shown by the dotted lines, subtracting the MISR ground biases from the SMV-CMV differences largely eliminated cross-swath variations, leaving only a constant mean discrepancy. We note that cross-swath variations were not limited to MISR wind retrievals but were also observed in high-resolution (1.1 km) MISR CTHs. Both wind-corrected ("bestwind") and raw ("zerowind") CTHs were affected, although the amplitude of variation was only ∼100 m for the latter [*Ludewig*, 2010].

[82] Prompted by our findings, the MISR instrument team conducted a thorough investigation into the cause of the cross-swath dependency. The cross-swath artifact was eventually traced back to sub-pixel co-registration errors in the B and D cameras due to the MISR Camera Geometric Model not accounting for focal plane distortions correctly (V. Jovanovic, personal communication, 2011). We emphasize that MISR geolocation and co-registration accuracies were well within design specifications for all nine cameras [*Jovanovic et al.*, 2007]. The issue of systematically varying focal plane distortion errors was also recognized during routine quality monitoring; however, it was considered a marginal effect in most MISR products due to its very small, few tenths of a pixel, magnitude. The fact that such sub-pixel uncertainties can cause systematic and measurable biases in SMVs underlines the utmost importance of highly accurate georectification for stereo wind retrievals. In order to avoid the arduous task of rewriting the Camera Geometric Model, the cross-swath artifact will be removed by applying sub-pixel georectification corrections at Level 2 processing in the next MISR production cycle. Such corrections will hopefully mitigate the overwhelmingly negative SMV-CMV mean wind differences as well.

4.7. Marine Stratocumulus Case Study

[83] As discussed in section 4.4, SMV heights were on average 0.5–1.0 km larger than CMV heights in the western basin of the South Atlantic off Brazil (see Figure 8c). Visual analysis of several MISR orbits suggested that these differences were partly caused by a low bias in CMV heights over boundary layer clouds. Here, a particular case is analyzed in detail as an example. We focused on blocks 107–118 from MISR orbit 46033 (path 192) collected on 13 August 2008, when Meteosat-9 imagery showed an extensive marine stratocumulus field covering large sections of the South Atlantic throughout the entire day. The collocated SMVs and CMVs were in excellent agreement in terms of wind speed and direction, however, SMVs were consistently assigned 1 km or more above CMVs. The very small vector differences ruled out MISR N-S wind component errors as a possible explanation for such large height discrepancies. To gain further insights, we compared SMV and CMV heights

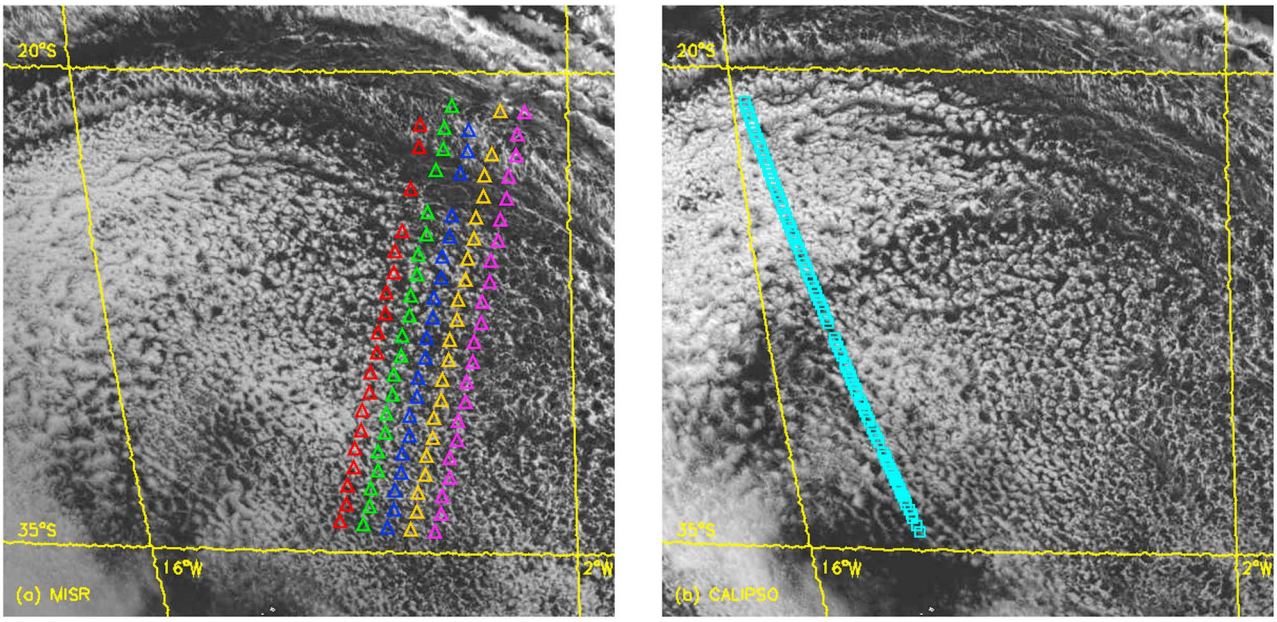

Figure 13. Meteosat-9 SEVIRI image of our case study area on 13 August 2008 for (a) MISR overpass at 10:27 UTC and (b) CALIPSO overpass at 14:57 UTC. In Figure 13a, triangles mark MISR SMV locations for path 192, orbit 46033, blocks 107-118 with red, green, blue, orange, and magenta corresponding to cross-swath domain index 2 to 6, respectively. In Figure 13b, cyan squares mark the locations of CALIPSO measurements from data file CAL_LID_L2_01kmCLay-ValStage1-V3-01.2008-08-13T14-45-35ZD.

with boundary layer heights (BLHs) and cloud boundaries from the ERA-Interim reanalysis. CMV heights were additionally compared to lidar cloud top heights (CTHs) and cloud base heights (CBHs) along the nearest CALIPSO track, occurring ∼4 h after the MISR overpass.

[84] Figure 13 indicates the locations of the MISR swath and CALIPSO track overlaid on the corresponding Meteosat-9 visible image. As shown, MISR sampled the eastern part of the cloud field characterized by broken, open cell structures, while CALIPSO flew over more contiguous and thicker clouds in the western part of the domain. The comparison of SMV and CMV heights with reanalysis BLHs and cloud boundaries is given in Figure 14a and that of CMV heights with CALIPSO CTHs and CBHs as well as reanalysis BLHs and cloud boundaries is plotted in Figure 14b. In reanalysis data, we defined cloud volume as liquid water content exceeding 0.01 g/kg.

[85] Model boundary layer heights were at 1.5 ± 0.2 km at most locations and times, underlying the stable and persistent nature of large-scale meteorological conditions in the study area. Over the MISR swath, the forecasted cloud top boundaries were typically 300–600 m above the diagnosed boundary layer. The SMV heights agreed well with model BLHs in the southern part of the swath, but they were increasingly above it moving north. Nevertheless, MISR stereo heights were always within or very close to the forecasted cloud boundaries. Along the CALIPSO track, where clouds were thicker and less broken, the agreement between model data and observations was even better. Reanalysis BLHs agreed particularly well with lidar CTHs. In addition, the forecasted cloud boundaries were also only ∼200 m (or ∼10 hPa) higher than the corresponding lidar CTHs and CBHs.

[86] Some model-observation differences and model inconsistencies were expected due to the difficulties representing stratocumulus clouds in forecast models. The ECMWF model is known to produce a generally too shallow boundary layer and clouds that are often located above the mixed layer [*Stevens et al.*, 2007; *Hannay et al.*, 2009]. The rather coarse 1.5° resolution of reanalysis fields also introduced differences in comparison to high-resolution satellite observations. Given these limitations, we found the agreement between ECMWF reanalysis data and MISR SMV heights and CALIPSO CTHs and CBHs remarkably good.

[87] A caveat to notice is the apparent cross-swath dependence of SMV heights. In Figure 14a, MISR heights along a given cross-track segment were connected by lines and colored according to their cross-swath position. The stereo heights showed the same cross-swath variation as in section 4.6 (see Figure 12), that is, values at the western edge of the swath (red and green) were usually lower than ones at the eastern edge (orange and magenta). The SMV-CMV differences in N-S wind also had a cross-swath dependence with a magnitude of ∼2 m s^{-1}, which would translate to MISR height variations of ∼160 m. Because the east-west height difference in this particular cloud field was typically larger, varying between 250 and 750 m, we concluded that part of it was real.

[88] Compared to MISR, CALIPSO, and reanalysis cloud heights Meteosat-9 heights appeared much too low. The CMVs used the EBBT method and were mostly assigned to elevations between 200 and 500 m, except in the latitude range 26°S–23°S where they reached altitudes between 800 and 1200 m. We emphasize that in our study area somewhat lowered CMV heights were expected, because the Meteosat-9 algorithm assigns stratocumulus wind vectors

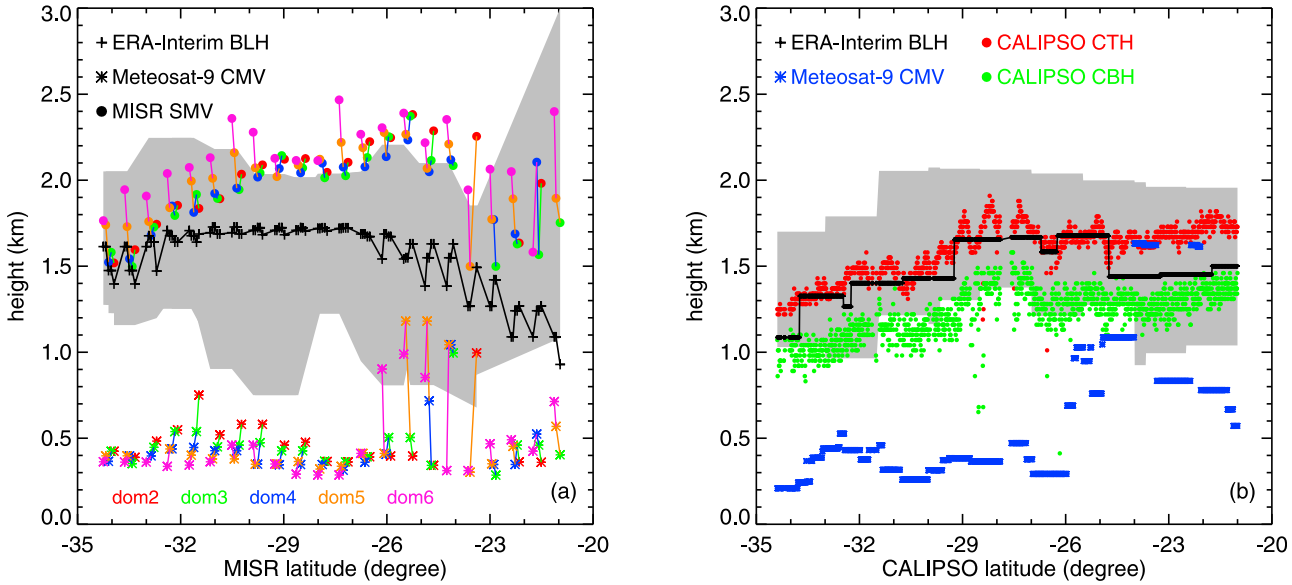

Figure 14. Height comparison along (a) the MISR track and (b) the CALIPSO track shown in Figure 13. In Figure 14a, the Meteosat-9 CMV heights (asterisks) and MISR SMV heights (filled circles) are color coded according to MISR cross-swath domain index. In Figure 14b, filled red and green circles correspond to CALIPSO cloud-top heights (CTH) and cloud-base heights (CBH), respectively. Also shown are ERA-Interim boundary layer heights (BLH, black plus signs) and cloud volume with liquid water content >0.01 g/kg (gray shading).

closer to cloud base where they are more representative of the flow and have a larger forecast impact. In boundary layer clouds, one of two possible corrections is applied to EBBT heights as discussed in section 2.2. In case of low-level temperature inversions, which are very common in the South Atlantic, CMV heights are forced to the level of inversion. In areas without a temperature inversion, on the other hand, a cloud base-height correction is applied to CMVs.

[89] Most CMV heights still appeared too low, as they were typically 1 km below reanalysis BLHs and 0.5–1.0 km below CALIPSO CBHs. Visual analysis of a large number of broken cloud scenes revealed an inverse correlation between the magnitude of the CMV height bias and cloud fraction, suggesting contributions from the warm sea surface to the observed brightness temperatures as the likely explanation. This result agreed with earlier studies, which also found that EBBT height biases due to sub-pixel clouds were negative and increased with decreasing cloud amount [*Schreiner and Menzel*, 2002; *Forsythe and Doutriaux-Boucher*, 2005]. The forecast impact of such height biases, however, is expected to be small, because wind shear is usually weak beneath the inversion level. Nevertheless, these findings indicated that CMV height assignment could be further improved using reanalysis data or independent retrievals such as MISR and CALIPSO.

5. Summary and Discussion

[90] One year of stereo motion vectors (SMVs) from the polar-orbiting MISR instrument were compared with collocated cloud-motion vectors (CMVs) from the geostationary Meteosat-9 satellite as part of the ongoing validation of MISR cloud products. Because the stereo wind algorithm did not apply a priori target selection, we first evaluated MISR cloud-free ground retrievals, expected to return near-zero wind and the height of topography. Such ground retrievals established minimum SMV RMS errors for E-W wind, N-S wind, and height of 0.7 m s^{-1}, 2 m s^{-1}, and 331 m, in good agreement with prelaunch estimates. They also showed that SMV uncertainties were significantly larger in the N-S (along-track) direction than in the E-W (cross-track) direction due to strong coupling between cloud motion and height along the MISR track, which had a sensitivity of −82 m height error per 1 m s^{-1} N-S wind error.

[91] The orientation of ground vectors was not random but favored the 14°/194° heading of the Terra satellite, which we could explain by retrieval sensitivities to tracking location errors. The distinct orientation of ground retrievals allowed us to filter them out from the subsequent SMV-CMV comparison. We also discovered apparent cross-swath variations in SMV E-W wind, N-S wind, and height with a magnitude of 0.6 m s^{-1}, 2.6 m s^{-1}, and 210 m, respectively. Cross-swath variations were traced back to sub-pixel co-registration errors in B and D camera imagery caused by known focal plane distortions that were previously deemed insignificant to take into account (V. Jovanovic, personal communication, 2011). In sum, ground retrievals proved useful to evaluate the overall accuracy of MISR co-registration and establish lower limits on SMV uncertainties; therefore, we recommend retaining them in the stereo product. However, such cloud-free retrievals need to be explicitly flagged in future updates to avoid their inclusion in validation or assimilation studies.

[92] For cloud targets, a significant shortcoming of the MISR data set was the considerably lower coverage of high-quality (WQ ≥ 3) SMVs compared to high-quality (QI ≥ 80) CMVs: 42% versus 78%. SMVs were also heavily dominated by low-level retrievals, in contrast to the more even

vertical distribution of CMVs. The comparison between high-quality observations tended to be better over ocean than land and showed negative mean differences for both wind components in most areas and through the entire troposphere, that is, SMVs had generally weaker westerlies and southerlies than CMVs. The full-disk-average SMV-CMV difference and rmsd in E-W wind were -0.4 m s^{-1}, -1.0 m s^{-1}, -0.7 m s^{-1} and 2.4 m s^{-1}, 3.8 m s^{-1}, 3.5 m s^{-1} for low- (>700 hPa), mid- (700–400 hPa), and high-level (<400 hPa) clouds, respectively. The corresponding N-S wind mean difference and rmsd showed a much stronger increase with height, being -0.8 m s^{-1}, -2.9 m s^{-1}, -4.4 m s^{-1} and 3.5 m s^{-1}, 6.9 m s^{-1}, 9.5 m s^{-1}, respectively, at low, mid, and high levels. These results were in general agreement with previous comparison studies [*Davies et al.*, 2007; *Hinkelman et al.*, 2009].

[93] We found the best overall agreement between SMVs and CMVs in marine stratocumulus off Namibia, with a small mean difference and rmsd near the theoretical minimum MISR uncertainty in both wind components. The largest differences occurred in convective cloud regimes or generally in the Tropics. The MISR algorithm has known difficulties in rapidly developing clouds due to stereo matching uncertainties or the breakdown of the assumption of no vertical cloud motion. However, CMVs are also more error-prone at low latitudes, as indicated by the blacklisting of geostationary winds between 25°S–25°N in the ECMWF assimilation system. Therefore, the larger tropical differences probably reflected increased uncertainties in both data sets. The MISR cross-swath bias found in ground retrievals was also evident in the SMV-CMV comparison, that is, SMVs were less accurate on the eastern side of the MISR swath than on the western side.

[94] The most challenging part of the comparison was the interpretation of height differences. The overall comparison statistics somewhat depended on the choice of height retrieval used for binning the data (MISR versus Meteosat-9), because wind pairs with large height differences could fall into different altitude categories (low, mid, high). Therefore, height differences had to be analyzed on a regional basis as well as for different cloud types in order to understand the mean results. When binned according to MISR heights, the mean height difference was positive at all levels, being largest for high-level clouds (∼700 m), smallest for mid-level clouds (∼270 m), and in between for low-level clouds (∼440 m). A regional analysis showed that low-level SMVs were assigned to higher altitudes than CMVs in most areas, except Brazil, Africa, and the southernmost Atlantic where SMV heights were on average lower. We also found that the relatively small mid-level mean height difference was due to partial cancellation of larger regional differences and the height rmsd was actually largest for this layer. For high-level clouds, regional differences were overwhelmingly positive.

[95] As a further step, we analyzed data clusters characterized by large differences in the SMV-CMV height scatterplot. Here, the most oblique MISR Df/Da cameras proved particularly useful to visually identify thin high-level cloud and aerosol layers. The most extreme height differences were usually artifacts, associated with multilevel clouds where the instruments tracked different layers. In the vast majority of such cases Meteosat-9 tracked the higher levels and MISR tracked the lower levels. However, in situations with low-level clouds underneath extensive cirrus or dust the opposite could happen, if the lower layers were completely obscured in the most oblique MISR views.

[96] We also identified several regions and cloud types where the large SMV-CMV height differences were due to genuine CMV retrieval biases. In thinner mid- and high-level clouds over Africa and Arabia, and also in broken marine boundary layer clouds the EBBT heights were often biased low due to radiance contributions from the warm surface. The latter case was further demonstrated by a detailed study of a South Atlantic marine stratocumulus field, where a comparison to ERA-Interim reanalysis data and CALIPSO lidar heights clearly indicated that the larger SMV heights were more accurate. In contrast, marine boundary layer CMVs could be erroneously assigned to mid levels by the CO_2-slicing method in multilayer situations. Such positive CMV height biases were often encountered in the South Atlantic.

[97] As suggested above, the comparison in areas with frequent multilayer clouds was affected by lack of imagery of the actually tracked cloud patches. This limitation of the operational data sets prevented us from filtering out wind pairs that corresponded to clouds at different levels. Future studies could perhaps minimize multilayer mismatches by storing and comparing images of tracked cloud targets in a dedicated research data set covering a limited time period. The impact of recent upgrades to the MISR algorithm, such as, replacement of the Nested Maxima feature matcher with a more accurate area matcher, inclusion of sub-pixel registration corrections, and higher spatial resolution retrievals also has to be thoroughly evaluated. Preliminary tests of the improved stereo algorithm have indicated largely reduced cross-swath bias as well as increased SMV coverage and quality (K. Mueller, personal communication, 2011).

[98] We finally note that from a data assimilation perspective, stereo height improvements are only relevant in the case of strong vertical wind shear. Evaluation of MISR's practical potential will therefore require a triple collocation approach similar to that of *Stoffelen* [1998], where SMVs and CMVs are not compared in isolation but with the help of model wind profiles. A further challenge will be the derivation of an SMV observation operator capable of handling assimilation of the strongly correlated along-track wind and height information. In our opinion, SMVs have forecast potential; however, their positive impact has yet to be demonstrated.

[99] **Acknowledgments.** The presented work was partially supported by the European Commission's Marie Curie Actions under grant agreement MIRG-CT-2007-208245. ERA-Interim reanalysis data were provided by ECMWF. We thank Catherine Moroney, Veljko Jovanovic, and Kevin Mueller of the Jet Propulsion Laboratory, California Institute of Technology, for their help with the MISR dataset, as well as Arthur de Smet and Régis Borde of EUMETSAT for details of the Meteosat-9 wind retrieval algorithm. Thanks also go to Iliana Genkova of the Royal Netherlands Meteorological Institute (KNMI) for helping us decode BUFR data and to Paul Poli of ECMWF for assistance with reanalysis products. Jan-Peter Muller of Mullard Space Science Center, University College London, and Ad Stoffelen of KNMI are acknowledged for stimulating discussions on future multi-angle wind retrieval concepts. We are grateful to the Max Planck Institute for Meteorology (MPI-M), Hamburg, for hosting K. Lonitz of the University of Leipzig during her master's project. We are also indebted to Johannes Quaas of MPI-M, who provided generous support to us through his Emmy Noether grant from the German Research Foundation

(DFG). Finally, the suggestions of four anonymous reviewers greatly improved the paper.

References

Bormann, N., and J.-N. Thépaut (2004), Impact of MODIS polar winds in ECMWF's 4DVAR data assimilation system, *Mon. Weather Rev.*, *132*, 929–940, doi:10.1175/1520-0493(2004)132<0929:IOMPWI>2.0.CO;2.

Cotton, J., and M. Forsythe (2010), Fourth analysis of the data displayed on the NWP SAF AMV monitoring website, *NWP SAF Tech. Doc. NWPSAF-MO-TR-024 Vers. 1.0*, Met Off., Reading, U. K.

Davies, R., Á. Horváth, C. Moroney, B. Zhang, and Y. Zhu (2007), Cloud motion vectors from MISR using sub-pixel enhancements, *Remote Sens. Environ.*, *107*(1–2), 194–199, doi:10.1016/j.rse.2006.09.023.

Dee, D. P., et al. (2011), The ERA-Interim reanalysis: Configuration and performance of the data assimilation system, *Q. J. R. Meteorol. Soc.*, *137*, 553–597, doi:10.1002/qj.828.

Diner, D. J., R. Davies, L. Di Girolamo, Á. Horváth, C. Moroney, J. P. Muller, S. Paradise, D. Wenkert, and J. Zong (1999), MISR Level 2 cloud detection and classification algorithm theoretical basis, *JPL Tech. Doc. D-11399, Rev. D*, Jet Propul. Lab., Calif. Inst. of Technol., Pasadena.

EUMETSAT (2011), Meteorological products extraction facility algorithm specification document, *EUM/MSG/SPE/022 v5A*, Darmstadt, Germany.

Forsythe, M., and M. Doutriaux-Boucher (2005), Second analysis of the data displayed on the NWP SAF AMV monitoring website, *NWP SAF Tech. Doc. NWPSAF-MO-TR-020 Vers. 1.3*, Met Off., Reading, U. K.

Forsythe, M., and R. Saunders (2008), Third analysis of the data displayed on the NWP SAF AMV monitoring website, *NWP SAF Tech. Doc. NWPSAF-MO-TR-022 Vers. 1.2*, Met Off., Reading, U. K.

Hannay, C., D. L. Williamson, J. J. Hack, J. T. Kiehl, J. G. Olson, S. A. Klein, C. S. Bretherton, and M. Köhler (2009), Evaluation of forecasted southeast Pacific stratocumulus in the NCAR, GFDL, and ECMWF models, *J. Clim.*, *22*, 2871–2889, doi:10.1175/2008JCLI2479.1.

Hinkelman, L. M., R. T. Marchand, and T. P. Ackerman (2009), Evaluation of Multiangle Imaging Spectroradiometer cloud motion vectors using NOAA radar wind profiler data, *J. Geophys. Res.*, *114*, D21207, doi:10.1029/2008JD011107.

Holmlund, K. (1998), The utilization of statistical properties of satellite-derived atmospheric motion vectors to derive quality indicators, *Weather Forecast.*, *13*(4), 1093–1104, doi:10.1175/1520-0434(1998)013<1093:TUOSPO>2.0.CO;2.

Holmlund, K., C. S. Velden, and M. Rohn (2001), Enhanced automated quality control applied to high-density satellite-derived winds, *Mon. Weather Rev.*, *129*(3), 517–529, doi:10.1175/1520-0493(2001)129<0517:EAQCAT>2.0.CO;2.

Holmlund, K., L. van de Berg, J. Gustafsson, A. de Smet, M. Carranza, G. Dew, and R. Borde (2010), Current status of EUMETSAT operational winds, paper presented at Tenth International Winds Workshop, Jpn. Meteorol. Agency, Tokyo.

Horváth, Á., and R. Davies (2001a), Feasibility and error analysis of cloud motion wind extraction from near-simultaneous multiangle MISR measurements, *J. Atmos. Oceanic Technol.*, *18*(4), 591–608, doi:10.1175/1520-0426(2001)018<0591:FAEAOC>2.0.CO;2.

Horváth, Á., and R. Davies (2001b), Simultaneous retrieval of cloud motion and height from polar-orbiter multiangle measurements, *Geophys. Res. Lett.*, *28*(15), 2915–2918, doi:10.1029/2001GL012951.

Jovanovic, V., C. Moroney, and D. Nelson (2007), Multi-angle geometric processing for globally geo-located and co-registered MISR image data, *Remote Sens. Environ.*, *107*(1–2), 22–32, doi:10.1016/j.rse.2006.08.013.

Key, J. R., D. Santek, C. S. Velden, N. Bormann, J.-N. Thépaut, L. P. Riishøjgaard, Y. Zhu, and W. P. Menzel (2003), Cloud-drift and water vapor winds in the polar regions from MODIS, *IEEE Trans. Geosci. Remote Sens.*, *41*, 482–492, doi:10.1109/TGRS.2002.808238.

Le Marshall, J., N. Pescod, A. Khaw, and G. Allen (1993), The real-time generation and application of cloud-drift winds in the Australian region, *Aust. Meteorol. Mag.*, *42*(3), 89–103.

Lewicki, S. A., and J. Zong (1999), MISR Level 1 ancillary geographic product algorithm theoretical basis, *JPL Tech. Doc. D-13400, Rev. A*, Jet Propul. Lab., Calif. Inst. of Technol., Pasadena.

Ludewig, E. (2010), Evaluation of satellite cloud-top height measurements along stratocumulus to cumulus transition trajectories: Multi-sensor analysis, Master's thesis, 128 pp., Univ. of Hamburg, Hamburg, Germany.

Marchand, R. T., T. P. Ackerman, and C. Moroney (2007), An assessment of Multiangle Imaging Spectroradiometer (MISR) stereo-derived cloud top heights and cloud top winds using ground-based radar, lidar, and microwave radiometers, *J. Geophys. Res.*, *112*, D06204, doi:10.1029/2006JD007091.

Moroney, C., Á. Horváth, and R. Davies (2002), Use of stereo-matching to coregister multiangle data from MISR, *IEEE Trans. Geosci. Remote Sens.*, *40*(7), 1541–1546, doi:10.1109/TGRS.2002.801146.

Mueller, K., M. J. Garay, L. Di Girolamo, V. Jovanovic, and C. Moroney (2010), MISR cloud motion vector product algorithm theoretical basis, *JPL Tech. Doc. D-64973*, Jet Propul. Lab., Calif. Inst. of Technol., Pasadena.

Muller, J.-P., A. Mandanayake, C. Moroney, R. Davies, D. J. Diner, and S. Paradise (2002), MISR stereoscopic image matchers: Techniques and results, *IEEE Trans. Geosci. Remote Sens.*, *40*(7), 1547–1559, doi:10.1109/TGRS.2002.801160.

Nieman, S. J., J. Schmetz, and W. P. Menzel (1993), A comparison of several techniques to assign heights to cloud tracers, *J. Appl. Meteorol.*, *32*(9), 1559–1568, doi:10.1175/1520-0450(1993)032<1559:ACOSTT>2.0.CO;2.

Rohn, M., G. Kelly, and R. W. Saunders (2001), Impact of a new cloud motion wind product from Meteosat on NWP analyses and forecasts, *Mon. Weather Rev.*, *129*, 2392–2403, doi:10.1175/1520-0493(2001)129<2392:IOANCM>2.0.CO;2.

Schmetz, J., K. Holmlund, J. Hoffman, B. Strauss, B. Mason, V. Gaertner, A. Koch, and L. Vandeberg (1993), Operational cloud-motion winds from Meteosat infrared images, *J. Appl. Meteorol.*, *32*(7), 1206–1225, doi:10.1175/1520-0450(1993)032<1206:OCMWFM>2.0.CO;2.

Schreiner, A. J., and W. P. Menzel (2002), Comparison of cloud motion vector height assignment techniques using the GOES-12 imager, paper presented at Sixth International Winds Workshop, CIMSS, Madison, Wis.

Stevens, B. (2005), Atmospheric moist convection, *Annu. Rev. Earth Planet. Sci.*, *33*, 605–643, doi:10.1146/annurev.earth.33.092203.122658.

Stevens, B., A. Beljaars, S. Bordoni, C. Holloway, M. Köhler, S. Krueger, V. Savic-Jovcic, and Y. Zhang (2007), On the structure of the lower troposphere in the summertime stratocumulus regime of the northeast Pacific, *Mon. Weather Rev.*, *135*, 985–1005, doi:10.1175/MWR3427.1.

Stoffelen, A. (1998), Toward the true near-surface wind speed: Error modeling and calibration using triple collocation, *J. Geophys. Res.*, *103*(C4), 7755–7766, doi:10.1029/97JC03180.

Turner, J., and D. E. Warren (1989), Cloud track winds in the polar regions from sequences of AVHRR images, *Int. J. Remote Sens.*, *10*(4), 695–703, doi:10.1080/01431168908903911.

Velden, C. S., and K. Holmlund (1998), Report from the working group on verification and quality indices (WG III), paper presented at Fourth International Winds Workshop, EUMETSAT, Saanenmöser, Switzerland.

Á. Horváth, Remote Sensing Group, Physics Department, Leibniz Institute for Tropospheric Research, Permoserstrasse 15, D-04318 Leipzig, Germany. (akos.horvath@tropos.de)

K. Lonitz, Atmosphere in the Earth System, Max Planck Institute for Meteorology, Bundesstrasse 53, D-20146 Hamburg, Germany. (katrin.lonitz@zmaw.de)